UNIVERSITY OF NAPOLI FEDERICO II

Doctorate School in Molecular Medicine

Doctorate Program in
Genetics and Molecular Medicine
Coordinator: Prof. Lucio Nitsch
XXV Cycle

"Myc-mediated transcription control of SAE1 and PUMA loci in cancer and reprogramming"

MIRIAM LUBRANO LAVADERA

Napoli 2013

Table of contents

List of publications

Amente S, Zhang J, Lubrano Lavadera M, Lania L, Avvedimento EV, Majello B. **Myc and PI3K/AKT signaling cooperatively repress FOXO3a-dependent PUMA and GADD45a gene expression.**
Nucleic Acids Res 2011: 39(22): 9498-507.

Amente S, Lubrano Lavadera M, Di Palo G, Majello B.
SUMO-activating SAE1 transcription is positively regulated by Myc
Am J Cancer Res. 2012: 2(3): 330-4.

Abstract

The Myc oncogene is the most studied transcription factor in biology. It plays an important role in development and cancer biology regulating cell cycle and apoptosis. The Myc oncogene is also implicated in a variety of other cellular processes such as self-renewal, differentiation and reprogramming in which its involvement is less understood. Despite growing evidence linking increase of Myc protein to stem-like phenotypes in cancer, the mechanism underlying Myc's contribution to the acquisition of "stemness" at a molecular level it is not yet clear.

To regulate its target genes, Myc binds to a specific sequence within DNA and mostly acts as a transcriptional activator. However, Myc down-regulates a small number of genes including PUMA and GADD45a the activity of which relies also upon FOXO3a transcription factor. In this study we have attempted *i)* to delineate the crosstalk between the Myc and FOXO3a pathways and *ii)* to suggest a molecular mechanism linking the increase of Myc protein and the consequent activation of its target genes to cell reprogramming.

The RAT and hT-RPE cell lines expressing a 4-hydroxytamoxifen-inducible MycER chimera have been used to address the first task, demonstrating that following induction, Myc is rapidly recruited to PUMA and GADD45a. Furthermore, a concomitant switch in promoter occupancy from FOXO3a to PUMA was observed. Myc recruitment stimulates deacetylation of H3 and H4 histones and methylation of the lysine 9 in H3 on both PUMA and GADD45a promoters leading to their downregulation. PUMA is a close neighbor of SUMO-activating enzyme 1 (SAE1) and whilst studying the regulation of PUMA, we observed a peak of RNA polymerase II in the second intron of the PUMA gene, responsible for activation of SAE1. We found that Myc activates SAE1 transcription via direct binding to canonical E-boxes in the vicinity of its transcription start site. The downregulation of PUMA and GADD45a and the up-regulation of SAE1 have also been seen in the heterogeneous primary murine mammary progenitor cells following their reprogramming into stem cells induced by Myc. On the contrary, when expression of Myc leads to the acquisition of 'stemness' within a homogeneous population of murine progenitor cells we observed up-regulation of PUMA while SAE1 was not affected, suggesting that in these cells the regulation of PUMA remains under the transcriptional control of p53.

Taken together, our data highlight a role for Myc in cell growth via the specific inhibition of FOXO3a-dependent transcription of PUMA and GADD45a and add a new insight in the context of Myc-driven oncogenesis. In fact,we show that, at least during Myc-mediated reprogramming of heterogeneous primary murine mammary progenitor cells, Myc activates directly SAE1 transcription. The activation of SAE1 has been previously shown by others as necessary for cancerous transformation.

Introduction

1.1 c-Myc and its physiological function

The *Myc* proto-oncogene family (comprising c-myc, N-myc and L-myc) is the most exhaustively studied group of genes in biology. In its physiological role, Myc is widely expressed during embryogenesis and in tissue compartments of the adult that possess high proliferative capacity (Pelengaris et al. 2002). Myc promotes cell growth and proliferation while concomitantly also functioning to inhibit terminal differentiation of most cell types and to sensitize cells to apoptosis (Pelengaris et al. 2002). Myc is a basic helix-loop-helix zipper (bHLHZ) protein that heterodimerizes with the small bHLHz protein Max and binds the E-box sequence CACGTG (Eilers et al. 2008). The binding of Myc-Max complex at the E-box region has been associated with gene activation, but Myc has been also implicated in the context of transcriptional repression (Eilers et al. 2008). Given Myc's role in gene activation and repression, gene expression profiling has been employed widely to examine the effects of Myc overexpression in a wide range of biological settings. The emerging trend from all of these studies indicates that Myc overexpression influences the regulation of genes that, collectively, comprise a broad range of biological functions (Patel et al. 2004b). The majority of up-regulated genes are involved in cell growth and more specifically, in ribosome biogenesis, protein synthesis and metabolism. While many growth-related genes are activated following Myc-expression, a few genes are down-regulated by Myc. These down-regulated genes are involved in cell cycle arrest, cell adhesion, and cell-cell communication. Given this ability to simultaneously control such contrasting cellular functions, Myc becomes a crucial mediator of normal development (Zindy et al. 2006) and tumorigenesis (Seoane et al.2002; Oskarsson et al. 2006). Therefore, when deregulated Myc may drive the limitless replicative potential characteristic of nearly all tumors (Hanahan and Weinberg 2000). Recently, the cell-cycle effects of ablating Myc have been investigated. Loss of Myc function in a rat fibroblast cell line shows greatly reduced rates of cell proliferation, accompanied by cell-cycle defects in G1 (Mateyak et al. 1997). The first notion that Myc influenced cell growth arises from the correlation between Myc and the expression of the rate-limiting translation initiation factors eIF4E and eIF2a, which are now considered to be direct Myc targets (Eilers et al. 2008). Several important studies show the insights into how Myc might promote cell proliferation, revealing the ability of Myc to activate or repress target genes that are involved in cell cycle progression. Indeed, Myc induces cyclin-E-CDK2 activity early in the G1 phase of the cell cycle, highlighting the relevant role of Myc in G1-S progression (Steiner et al. 1995, Berns et al. 1997). Furthermore, Myc regulates

expression of the CCND2 gene (encoding cyclin D2) and CDK4, that are able to sequester the CDK inhibitor KIP1 in cyclin-D2-CDK4 complexes (Bouchard et al. 1999, Hermeking et al. 2000).

Studies supporting the idea that Myc might also exert important influences on the cell-cycle by repressing genes, show that the CDK inhibitors p15 and p21, which are involved in cell-cycle arrest, are inactivated upon interaction of the Myc-Max complex with the transcription factor MIZ1. This prevents the association of MIZ1 with its own co-activator p300, and thus p15 and p21 cannot be transcriptionally activated (Staller et al. 2001, Herold et al. 2002).

Another confounding factor which must be considered when studying Myc in different systems is that its function appears to be not only cell type specific but also context dependent. This was demonstrated in an elegant study by Lawlor et al. (2006) showing, through the expression profiling of murine pancreatic B-cells following acute Myc induction, a wave of gene activation and repression over time. While many of these Myc regulated genes are, as expected, involved in growth, cell cycle progression and metabolism, a significant subpopulation of the affected genes had not been identified previously as regulated by Myc in other profiling experiments. While the expression profiling studies provide a basis for understanding Myc's broad effect on cells, which Myc targets are essential in a given cellular or biological context remains an open question. Indeed, the studies comparing binding with expression arrays show that a significant percentage of bound loci are also modulated at the transcriptional level when Myc abundance is altered (Zeller et al. 2006). However, although Myc binding is clearly coupled to transcription, there are a significant number of binding sites that are not directly associated with gene expression (Zeller et al. 2006). These sites may represent genes that are regulated contingently, dependent on a specific cell or developmental context, as previously mentioned.

In recent years a non-transcriptional role for Myc in regulating gene function has emerged. Dominguez and colleagues demonstrated that Myc can bind to and stimulate origins of DNA replication, independent of Myc transcriptional function (Dominguez-Sola et al. 2007), highlighting the notion that the presumed non-productive Myc binding sites could be replication origins (Eilers et Eisenman 2008). An important recent analysis asked whether specific histone modifications correlate with genomic Myc binding and found that elevated H3-K4 and H3-K79 methylation and core histone acetylation (active marks) are characteristic of Myc binding sites (Guccione et al. 2006). These marks are associated with open chromatin and suggest that Myc finds its target promoters when the chromatin is primed for gene transcription (Lüscher et al. 2011). Although Myc induction was not associated with an increase in H3K4me3, a modification associated with active promoters (Kouzarides et al. 2007), the inhibitory activity of Myc on lysine demethylases (KDMs) may be important to maintain H3K4me3 levels (Lüscher et al. 2011).

Furthermore, the association between Myc and the co-activator TRRAP (transformation/transcription domain associated protein) and their recruitment

to specific loci results in the preferential acetylation of histone H4 at a single nucleosome (Bouchard et al. 2001). This would alter chromatin structure to allow accessibility and binding of Myc-MAX complexes to target DNA sequences thereby modulating gene activation. Changes in histone acetylation were also observed in studies of genome wide approaches, in which Myc expression appeared to induce core histone acetylation at many different loci (Frank et al. 2001).

1.2 Myc-induced apoptosis

It is now widely acknowledged that putative cancer cells must avoid apoptosis for tumor growth, indeed the net expansion of a clone of transformed cells is not only achieved by an increased proliferative index, but also decreased apoptotic rate. Ectopic expression of Myc in fibroblasts cultured in the absence of survival factors, leads to apoptosis, highlighting the possibility of Myc to possess apoptotic activity (Evan et al.1992). Although interpreted by some as a conflict of growth signals - oncogenes activate apoptosis if the proliferative pathway is blocked in some way - the most widely held view of oncoprotein induced apoptosis is that the induction of cell-cycle entry sensitizes the cell to apoptosis: cell-proliferative and apoptotic pathways are coupled (Pelengaris et al. 2002). Interestingly, stimulation of apoptosis by Myc may not always be a direct effect linked to cell cycling, but can also arise through indirect actions that culminate in DNA damage. Several publications link Myc to the accumulation of reactive oxygen species via E2F1-mediated inhibition of nuclear factor of kB, though the consequences, either apoptosis or growth arrest, might be crucially dependent on cell type (Tanaka et al. 2002, Vafa et al. 2002). The first insight into Myc's role in apoptosis came from studies showing that Myc could induce the release of cytochrome c from mitochondria during apoptosis (Juin et al. 1998), causing the formation of apoptosome, and determining the caspase cascade (Pelengaris et al. 2002). Although the precise mechanism that is involved in Myc-mediated cytochrome release is unclear, Soucie et al. (2001) show that Myc is essential for activation of the proapoptotic BAX protein and subsequent cytochrome c release. Otherwise, the insulin-like growth factor 1 (IGF1) survival factor, inhibits Myc-induced apoptosis, in vitro, blocking cytochrome c release (Juin et al. 1998). In this scenario, it is important to consider that, the balance of anti- and proapoptotic molecules that are present within a Myc-activated cell, determines whether it lives or dies. Another possible mechanism that links Myc and apoptosis is through its indirect activation of p53 via ARF (Zindy et al. 1998). The importance of ARF in Myc-induced apoptosis was underscored in transgenic mice that expressed Myc only in B-lymphocytes and had lost one or both Bmi1 alleles. Given the role of Bmi1 in suppressing ARF and Ink4 a loss of expression therefore, inhibited Myc-induced lymphomagenesis by increasing Arf-dependent apoptosis (Jacobs et al. 1999). Taken together, these studies show that the mechanism by which Myc induces apoptosis may be dictated by cell type and moreover, it may be modified by the presence or absence of additional mutations in other pro- and anti apoptotic genes.

1.3 c-Myc inhibits cell differentiation

The ability of Myc to bind to a large number of genomic loci has been also demonstrated in ES cells (Kim et al. 2008). Indeed, Myc is part of the "magic quartet" of transcription factors that can reprogram somatic cells into induced pluripotent stem cells (iPSCs). Several studies found that ectopic expression of Myc augments the ability of Oct4, Sox2 and Klf4 to induce the formation of pluripotent cells from mouse and human fibroblast, liver cells, and mature B cells (Okita et al. 2007, Takahashi et al 2007, Werning et al. 2007, Hanna et al. 2008). Oct4 and Sox2 are required for reprogramming, but the combination of other reprogramming factors can be flexible. For example, another set of mediators (Oct4, Sox2, Lin28 and the pluripotency factor Nanog) has been shown to reprogram human somatic cells into iPSCs (Yu et al. 2007). The frequency of reprogramming of primary cells is very low even when all the required factors are expressed in most cells, indicating that there are barriers that block successful reprogramming. Overexpression of oncogenic factors such as Myc in somatic cells during reprogramming induce ARF/p53-dependent pathways, leading to senescence or apoptosis (Pelengaris et al. 2002). Therefore, p53 could be a crucial barrier to induced pluripotency. This idea was supported by several studies reporting a great increase in the reprogramming frequency of p53-deficient mouse and human fibroblasts when compared to their WT counterpart (Zhao et al. 2008, Kawamura et al. 2008, Marion et al. 2009, Utikal et al. 2009). Moreover, the elimination of ARF, a potent activator of p53 in response to oncogenic stress, also increases the reprogramming efficiency, further implicating p53 as an important barrier controlling reprogramming (Li et al. 2009). iPS cells generated from p53 null mouse fibroblasts form tumors when injected into mice suggesting effects on genomic integrity and offering at least one general explanation for the low frequency of iPS generation during reprogramming (Hong et al. 2009). In fact, all molecules involved in iPS have some oncogenic potential, indeed Klf4, as Myc, is a well known oncoprotein. Several studies have shown the oncogenic potential of Nanog, Oct4, Lin 28 and Sox2 (Pelengaris et al. 2002, Almstrup et al. 2004, Hart et al. 2005). Pasi et al. (2011) confirmed the acquisition of genomic alterations (deletions and amplifications) in induced stem cells during reprogramming using several different experimental systems. The aberrations reported were suggestive of oncogene-induced DNA replication stress and were to a significant degree dependent on c-Myc expression. Taken together, these data suggest an explanation for why p53 inactivation facilitates stem cell reprogramming. The combination of overexpression of reprogramming factors, such as Myc, and inactivation of p53 in human cancer cells would provide the necessary components for the dedifferentiation of cancer cells, which might become cancer stem cells. In a physiological setting, Myc is essential for controlling the balance between self-renewal and differentiation of many adult stem cell types such as hematopoietic, mammary and intestinal stem cells (Wilson et al, Laurenti et al. 2012). Not surprisingly, Myc is also strongly implicated in the malignant counterpart for almost all of these adult systems

(Reavie et al. 2013, Orkin et al. 2011). Numerous experiments document the ability of Myc to inhibit terminal differentiation of multiple cell types in culture and to promote tumorigenesis in vivo when expressed in differentiated cells. In a number of cases, the resulting tumors have been transplanted, thus demonstrating the presence of tumor cells that are capable of self-renewal such as Myc-induced lymphomas and liver tumors (Shachaf et al. 2004, Giurato et al. 2006). Moreover, since high levels of Myc perturb terminal differentiation and enhance self-renewal of some committed and differentiated cells, one might expect that during tumor progression Myc could promote the formation of cancer-initiating cells that retain developmental plasticity but differ from their normal stem cell counterpart. The expression of Myc in hematopoietic stem cells (HSCs) leads to the rapid formation of pre B-cell lymphomas if apoptosis is blocked by coexpression of Bcl-2. Cells derived from these lymphomas can be differentiated into either B-lymphocytes or macrophages in vitro suggesting that Myc induces the expression, in differentiated cells, of a gene subset that resembles the expression signatures of ES cells (Wong et al. 2008). In differentiated cells, whether Myc activates a subset of genes closely resembling an ESC signature or a few factors important for maintaining adult stemness is not yet clear (Orkin et al. 2011). The relationship between neoplastic cells and normal stem cells represents currently a question of top interest. The apparent parallels between the pathways required by tumor and normal stem cells have generated great interest in unraveling the mechanisms that regulate stemness in physiological and malignant contexts. The self-renewal and differentiation capacity of stem cells mirrors the high proliferative capacity and phenotypic plasticity of tumor cells. Recently, the identification of genes vital to support Myc-addicted tumors through a genome wide genetic screen for Myc-synthetic lethal (MySL) shRNAs in human mammary epithelial cells has been reported (Kessler et al. 2012, Evan et al. 2012). The most significant candidates identified in this study are the SAE1 and SAE2 genes whose products associate to form the heterodimer that is a critical component of the SUMO activating enzyme needed for SUMO conjugation to proteins (Hay et al. 2005). Most importantly, SAE depleted cells with high levels of Myc expression were impaired in their ability to form a correct mitotic spindle and consequently induced apoptosis. These results highlighted the crucial role of SAE1/2 gene expression in protecting cells from Myc-induced genomic instability. Intriguingly, SAE1 is located very close to the proapoptotic PUMA (p53 up-regulated modulator of apoptosis) gene on the human chromosome 19, with conserved synteny in mouse chromosome 7.

1.4 PUMA: p53 upregulated modulator of apoptosis

PUMA is a critical mediator of apoptosis induced by a variety of stimuli. PUMA encodes a BH3 only protein that functions as a proapoptotic gene triggering programmed cell death as a direct activator BAX and BAK that mediates cytochrome c release and caspase activation. PUMA induction is mediated in a p53-dependent and independent manner. PUMA activation by DNA damage is dependent by a functional p53 and mediated by a p53-responsive element in its promoter (Kaeser and Iggo 2002; Wang et al. 2007). In many tumors escaping apoptosis in which p53 is mutated, deletion or methylation mediated inactivation of PUMA efficiently protects against apoptosis induced by either DNA damage or oncogene activation (Yu et al. 2006; Yu et al. 2001). The p53 tumor suppressor pathway limits oncogenesis by inducing cell cycle arrest or apoptosis. In more of half of human tumors these pathways are impaired due to mutation in the p53 locus and inactivation of PUMA in a p53 independent manner is the only choice to activate the apoptotic pathway (Yu et al. 2001). It is expected that tumors inactivate p53 independent PUMA expression in order to gain cellular growth advantages. It is intriguing that approximately 40% of primary human Burkitt lymphomas (BLs), in which growth advantage is due to Myc oncogene over-expression, express mutant p53, and undetectable PUMA levels due to DNA hypermethylation and or inactive histone marks (H3K9me2) of the PUMA locus (Garrison et al. 2008). These finding suggest an inverse correlation of Myc and PUMA expression. PUMA is normally expressed at low levels and it is rapidly induced in response to stress signals (Yu et al. 2001). Binding sites for a multiple transcription factors in the PUMA regulatory regions have been found, and the functional role of p53, p73, Slug and FOXO3a in PUMA activation following stress in vivo have been investigated (Matallanas et al. 2007; Melino et al. 2004; Ming et al. 2008). In particular, FOXO3a-dependent regulation of PUMA in response to cytokine and growth factor withdrawal has been documented (You et al. 2006). Studies performed by large-scale chromatin immunoprecipitation (ChIP) have identified high affinity Myc binding E-boxes in the regulatory regions of PUMA. Moreover, clustering Myc target genes on the basis of histone modification marks, the PUMA E-boxes are characterized by high levels of histone methylation at H3K4me3, a pre-requisite for Myc binding and H3K9me2, which is generally considered a repressive mark. Since the functional relevance of Myc binding on PUMA E-boxes has not been addressed, here we report our investigation aimed at defining the functional role of Myc in regulating PUMA transcription.

Aim

Myc is overexpressed and/or activated in cancer. However, the full extent of the molecular mechanisms responsible for its action is not yet fully delineated. It is generally believed that the transcriptional rate of Myc targets is increased in most instances. However, despite this observation, a few negatively regulated targets have been identified over the years. Our laboratory has a long-standing interest in transcription modulation by Myc.

Considering that an overpowering majority of studies within the Myc field concentrates their research on the positively regulated Myc targets, we wanted to gain some insight into the regulation of two of the negatively controlled genes: PUMA and GADD45a. In particular, we were intrigued by the fact that the two genes are also targets of FOXO3a. Thus, to determine the extent of crosstalk between the Myc and FOXO3a pathways and investigate the biological significance of such interactions, we embarked upon the delineation of a mechanism that links transcriptional regulation by Myc and FOXO3a through PUMA and GADD45a.

As a serendipitous finding that we came across during this first part of the study, we identified a site of Pol II binding in the second intron of the PUMA gene. An investigation that followed showed that it was responsible for the transcription of PUMA's neighbor – SAE1, a gene otherwise implicated in Myc-mediated oncogenesis (Kessler et al. 2012). Therefore, we have focused our current study on regulation of the PUMA-SAE1 locus using different models of Myc induction. Specifically, we have manipulated Myc expression in several models of cancer and during "reprogramming" of murine mammary progenitors to a stem-like state with the scope of providing a molecular explanation for the phenomenon of synthetic lethality of Myc overexpression and SAE1/2 silencing.

Materials and Methods

3.1 Cell culture and drugs

RAT1 cells and hT-RPE expressing a 4-hydroxytamoxifen (OHT)-inducible MycER chimera (Littlewood et al. 1995), RAT1 and RAT-Myc$^{-/-}$ cells were cultured in DMEM medium supplemented with 10% fetal calf serum. Cells were made quiescent by contact inhibition followed by serum removal for 2 days. To induce entry into the cycle, synchronized growth-arrested cells were treated with OHT (1mM) alone or serum alone or OHT plus serum as indicated in the text and harvested at the indicated times. The AKT-inhibitor LY294002 (10mM) was added in the media where indicated. Growing RAT-MycER cells were treated with OHT for Myc induction (Myc) for 4h. OHT-treated and control-untreated cells were incubated with CPT (12 mM for 4 h) or Nutlin-3 (10 mM for 4 h) and prior to the quantification of PUMA and/or GADD45a mRNA levels by qPCR.

3.2 Transfections and siRNA

To carry out transient transfection experiments in RAT1 and RAT-MycER cells (Amente et al. 2010), we used MicroPoRATor Digital Bio Technology, a pipette-type electroporation. Indicated plasmids, DNAs or siRNA were introduced into each 3 X 10^6 dissociated cells in 100 ml volume according to manufacturer's instructions. Pulse width was determined according to applied voltages: 1400 V, 30 ms, 1 pulse. Electroporated cells were then seeded into 100-mm culture dishes containing 5 ml of culture media. After 5h of recovery, the cells were serum deprived for 48h. For siRNA treatments, ON-TARGETplus SMARTpool (L-003282- 00-0005) Myc; and ON-TARGETplus Non-targeting pool (D-001810-10-5) were obtained from Dharmacon. An amount of 100nM, final concentration of the pools, was used for each transfection. Expression of proteins was determined by western blot. In transfection experiments, RAT-MycER cells were transfected with the 3mg of FOXO3a-TM vector expressing a constitutively active FOXO3a by electroporation after 5h of recovery, the cells were serum deprived for 48h and mRNA levels were evaluated 1 and 4h after treatment with serum and OHT.

3.3 mRNA quantification by qPCR

cDNA was prepared from total RNA with the Quantitect Reverse Transcription Kit (Qiagen) according to manufactory's instructions. Each sample was assayed in triplicate. The qPCR data were normalized to the expression of the housekeeping b-glucuronidase (GUS) gene and after normalization the data were presented as fold change relative to the 0 point.

3.4 Quantitative chromatin immunoprecipitation

Following a wash with PBS, appropriate cells were cross-linked with a 1% formaldehyde/PBS solution for 5 min at room temperature. Cross-linking was stopped by adding glycine and samples were processed using the chromatin immunoprecipitation (ChIP) assay kit (Upstate Biotechnology) according to the manufacturer's protocol. Antibodies used in these experiments were as follows: c-Myc (N-262 Santa Cruz), anti-pol II monoclonal antibodies (8WG16, H14, H5, Covance), anti GADD45a (Santa Cruz), anti-H3K4me3, anti-H3K4me2, anti-H3K9me3, anti-H3K9me2 (Abcam), anti-H4Ac and H3Ac (Upstate). Immunoprecipitated untreated and input DNA values were used to subtract/normalize the values from ChIP samples. All values represent the average of at least three independent experiments. Untreated and input DNA values were used to subtract/normalize the values from qChIP samples according to the formula: % Input = 2^{DCt} 3; DCt = Ct (input)- Ct(cIP). qRT–PCR and qChIP data are presented as means of three at least independent experiment.

3.5 Induced mammary stem cells.

To prepare mammosphere cultures, mammary tissue from 5-month-old virgin female FVB mice (Harlan) were collected and dissociated mechanically. Disaggregation of the tissue was completed by enzymatic digestion in DMEM supplemented with 100 U/ml hyaluronidase (Sigma, St. Louis, MO, USA) and 200U/ml Collagenase (Sigma) for approximately 3 h at 37°C. The digested material was then centrifuged and filtered through 100, 70, 40 and 20uM meshes. Red blood cells were lysed by incubating the cell suspension in 0.2% NaCl. The resulting cells were plated on ultralow adhesion plates (Falcon, BD Biosciences, San Jose, CA, USA) at 100000 cells/ml in MEBM medium (BioWhittaker, Walkersville, MD, USA) supplemented with 5mg/ml insulin, 0.5mg/ml hydrocortisone, 2% B27 (Invitrogen, Carlsbad, CA, USA), 20ng/ml EGF and βFGF (BD Biosciences, San Jose, CA, USA) and 4mg/ml heparin (Sigma). Primary mammospheres were allowed to form for 6 days. At passaging, the number of mammospheres was counted, the mammospheres were then dissociated in single cells and the number of cells counted. A total of 5000 cells were then plated in 24-well plates.

Clearly, the number of mammospheres at each passage reflects the number of stem cells that had been plated, the rationale being that a stem cell can form a mammosphere, whereas, by definition, a progenitor cell cannot do it. In order to distinguish native stem cells from progenitor cells, primary mammary cells were stained with a lipophilic PKH26 dye (Sigma) for 5min. The reaction was blocked in 1% BSA and the cells were plated and passaged twice to obtain secondary mammospheres. Single cells obtained from disaggregated secondary mammospheres were sorted by flow cytometry on the basis of PKH26 fluorescence intensity (FACS Vantage SE flow cytometer, Becton and Dickinson, Franklin Lakes, NJ, USA). The PKH26-high population was

isolated as the most epifluorescent of the total population (about 1,7 % of the cells). PKH26-negative cells were gated at 10 times less fluorescence units with respect to the PKH26-high population (about 70% of the cells). Since stem cells divide once or just a few times during each passage, they retain high levels of the dye, whereas the progenitor cells that divide many times, become PKH-negative. Lentiviral infections were performed using the PWPI vector (Addgene, Cambridge, MA, USA) that contains the GFP reporter gene and either no other insert (Empty Vector) or MycER as an insert. Disaggregated primary mammospheres or PKH26-negative cells were plated in Phoenix-generated viral supernatant and infections were carried out in three cycles of 6h each. After 6 days of culture, secondary mammospheres were harvested, disaggregated and FACS sorted for the expression of GFP. For serial passage experiments, 5000 cells from disaggregated mammospheres were plated in 24-well plates and, after 6 days, counted, and replated at the same density. Treatment with 500nM OHT (Sigma) was performed for a range of duration of time after mammospheres formation (0, 4, 8, 24, 30hrs). Immunoblot analysis of protein extracts from mammosphere cultures was performed using anti-vinculin (Sigma), anti-phospho-serine15-p53 (Santa Cruz Biotechnology, Santa Cruz, CA, USA), primary antibodies, HRP conjugated secondary antibodies (Sigma) and the SuperSignal West Pico Substrate detection kit (Pierce, Rockford, IL, USA).

Results and Discussion

4.1 Myc and FOXO3a exert opposite control of PUMA transcription

4.1.1 Myc contributes to the repression of PUMA and GADD45a expression following growth stimulation

Since the functional relevance of Myc binding on PUMA E-boxes has not been addressed, here we report our investigation aimed at the definition of the functional role of Myc in regulating PUMA transcription.
To this end, we employed the RAT-MycER fibroblast cell line (Gargano et al. 2007) in which an inducible MycER protein is expressed upon treatment with 4-hydroxytamoxifen (OHT). The expression of PUMA and GADD45a was monitored in asynchronous RAT-MycER cells, and in cells that were serum-deprived for 2 days and then treated with OHT/serum. As expected, PUMA and GADD45a expression increased in response to growth factor deprivation, whilst their expression was inhibited following the serum-addition (Fig. 1A and 1B). In the absence of serum, the phosphoinositide 3-kinase PI3K/AKT pathway is inactive and FOXO3a remains unphosphorylated in the nucleus where it activates target genes (Accili et al. 2004, Brunet et al. 1999).
FOXO3a phosphorylation is inhibited by serum withdrawal but it is restored 4h after serum addition (Fig. 1A). Moreover, the presence of PI3-K inhibitor LY294002 or the overexpression of the constitutively active FOXO3a-TM prevents PUMA and GADD45a repression by serum (Fig. 1C). Collectively, these data indicate that activation of FOXO3a, in serum deprived RAT-MycER cells, stimulates the expression of PUMA and GADD45a. On the contrary, the cell growth stimulation by serum is accompanied by repression of their FOXO3a-dependent expression.
Utilizing the conditional expression of Myc in the RAT-MycER cells, we sought to determine the relative contribution of Myc to the repression of FOXO3a target genes. The silencing of Myc with specific siRNA restores PUMA and GADD45a expression to levels similar to those in serum-starved cells (Fig. 2A), whilst it reduces the expression of Nucleolin (NUC), a well-defined Myc-target (Amente et al. 2010). In serum starved cells, we did not detect significant differences in the relative levels of mRNA in samples treated with specific and control siRNAs suggesting that in such cells, the expression of both PUMA and GADD45a is mainly independent from Myc. To determine the relative contribution of serum and Myc activation to the repression of PUMA and GADD45a, we compared the relative levels of expression in cells that were treated with serum alone, OHT or serum–OHT together. We found that Myc is able to repress FOXO3a-target genes even in the absence of serum, although under these conditions the kinetics of the inhibition is slower (Fig. 2B).

However, serum does not fully substitute for Myc in the repression of PUMA and GADD45a. Indeed, the results obtained from RAT-Myc$^{-/-}$ cells show that the serum addition does not fully repress FOXO3a-targets (Fig. 2C). Moreover, a robust repression of PUMA and GADD45a mRNA levels were restored in RAT-Myc$^{-/-}$ transfected with Myc (Fig. 2C). To further investigate the endogenous Myc activity in response to serum addition, we monitored PUMA and GADD45a expression in RAT1 cells that were serum deprived for 2 days and then treated with serum for cell cycle re-entry. Upon addition of serum, the expression of both PUMA and GADD45a was inhibited, and most importantly silencing of endogenous Myc restored PUMA and GADD45a expression (Fig. 2D). Collectively, these results highlight a crucial role of Myc in the inhibition of FOXO3a-dependent gene expression in response to growth factor stimulation.

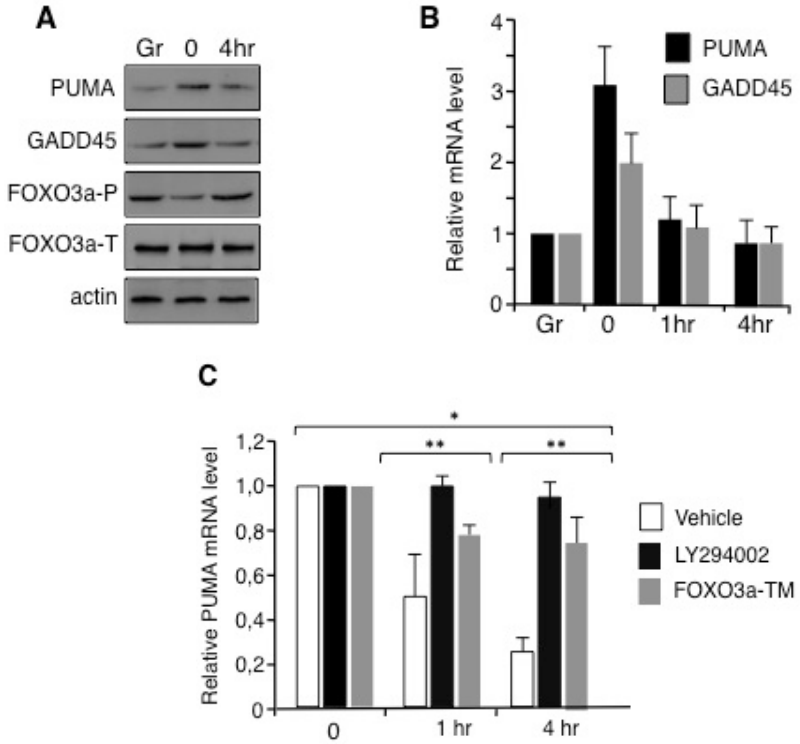

Figure 1. Myc inhibits FOXO3a-depeendent transcription. Asynchronous RAT-MycER growing cells (Gr) were serum deprived for 2 days (0) and then treated with serum and OHT for 4 h. (A) Protein expression is shown in immunoblots of whole-cell extracts with anti-PUMA, anti GADD45, anti-Phospho-FOXO3a, anti FOXO3a and anti actin for loading control. (B) mRNA expression levels of PUMA and GADD45a were quantified by qRT-PCR in asynchronous RAT-MycER growing cells (Gr), quiescent (0) and after 1 and 4 h of treatment with serum and OHT. mRNA levels were normalized to b-glucuronidase (GUS) mRNA levels. All values represent the average of at least three independent experiments. Error bars indicate SD. (C) RAT-MycER cells were transfected with the FOXO3a-TM vector expressing a constitutively active FOXO3a by electroporation as described; after 5h of recovery, the cells were serum deprived for 48 h and mRNA levels were evaluated 1 and 4 h after Myc induction in the presence of serum + OHT. The AKT-inhibitor LY294002 (10mM) was added to the media where indicated. mRNA expression was quantified by qRT–PCR and compared to quiescent cells. mRNA levels were normalized to b-glucuronidase (GUS) mRNA levels. All values represent the average +/- SD (n = 3). Error bars are standard error of the mean. *P < 0.05, **P < 0.01.

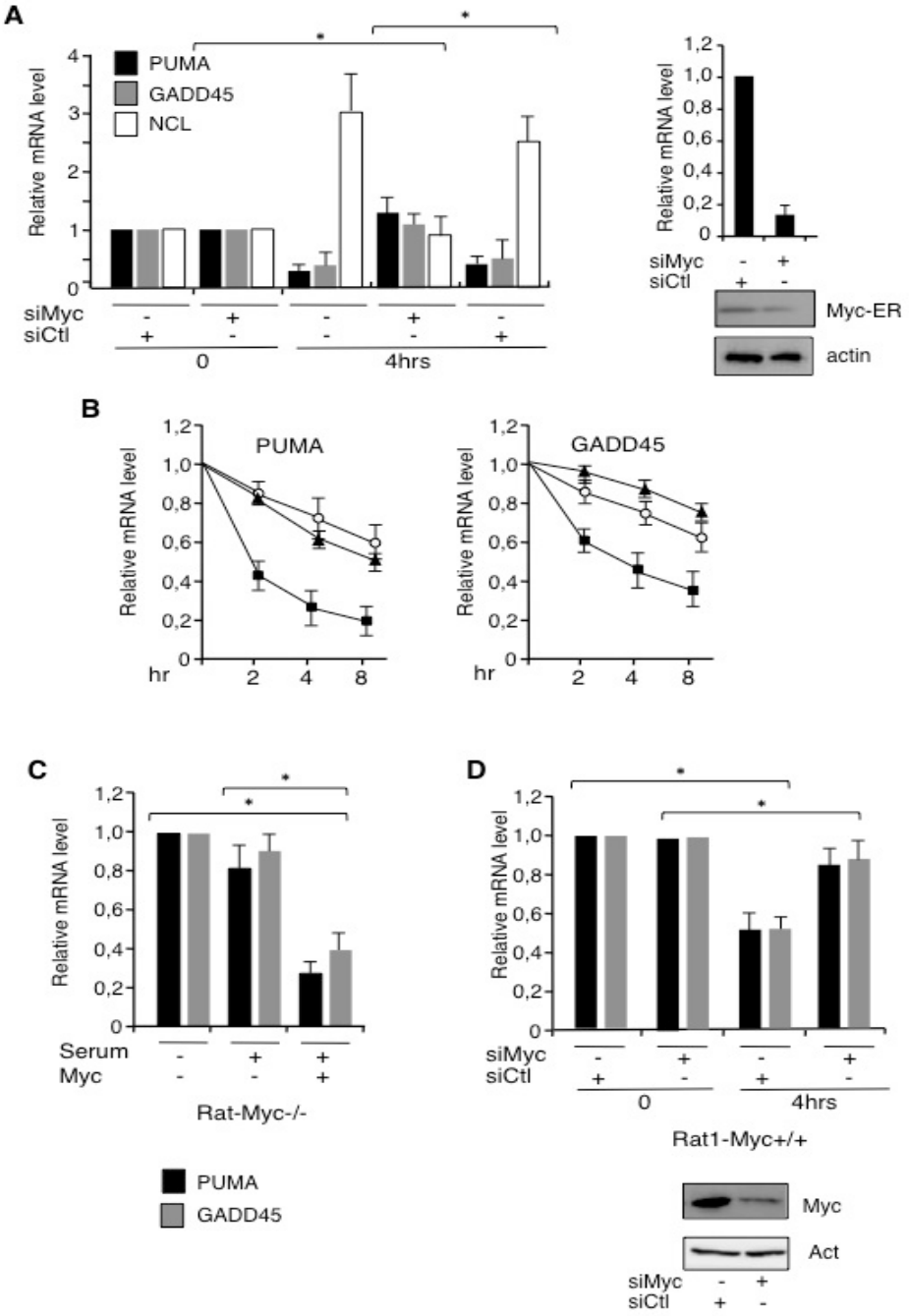

Figure 2. Myc knockdown prevents repression of FOXO3a targets. (**A**) Serum deprived RAT-MycER cells (0) were treated for 4h with OHT+ serum. Myc expression was inhibited with specific siRNA (siMyc) and siRNA non-targeting (siCtl) was used as scrambled RNAs. PUMA, GADD45a and NUC mRNAs expression levels were quantified by qRT–PCR. Error bars indicate SD (n=3). Error bars are standard error of the mean. *P < 0.05. The efficiency of Myc silencing by siRNA treatments measured by qRT–PCR and by immunoblot is shown on the right. (**B**) Quiescent RAT-MycER cells were stimulated with OHT+serum (black square), with OHT alone (empty circle) or with serum alone (black triangles) and expression levels of PUMA and GADD45a were quantified by reverse transcription and real-time PCR at the indicated times after treatment; values were compared to quiescent cells and presented as means of two independent experiments each analyzed by triplicate qRT–PCR. (**C**) RAT-Myc-/- cells as well as cells transfected with a Myc expression vector were serum deprived for 48 h and PUMA and GADD45a mRNA levels were evaluated by qRT–PCR 4 h after serum induction. Values were compared to quiescent cells. (**D**) Serum deprived (2 days) RAT1 cells (0) were treated with serum (10%) for 4h. Myc expression was inhibited with specific siRNA (siMyc) and siRNA non-targeting (siCtl) was used as scrambled RNAs. PUMA and GADD45 mRNAs expression levels were quantified by qRT–PCR. Error bars indicate +/- SD (n=3), *P<0.05. The efficiency of Myc silencing by siRNA treatments measured by immunoblot is shown on the bottom.

4.1.2 FOXO3a and Myc occupancy on PUMA and GADD45a chromatin is mutually exclusive

Previous reports showed that Myc represses GADD45a through binding to a sequence proximal to the promoter (Tran et al. 2002; Barsyte-Lovejoy, 2004), and several high affinity E-box sites have been mapped upstream of the ATG site of PUMA (Guccione et al. 2006; Yu and Zhang 2008), although a direct proof of Myc binding to these putative E-boxes has lacked. Large scale chromatin immunoprecipitation (ChIP) approach showed that PUMA contains high affinity E-box sites, suggesting it being a putative direct target of Myc. Moreover, clustering Myc target genes on the basis of histone modification marks, the PUMA E-boxes are characterized by high levels of histone methylation at H3K4me3, a pre-requisite for Myc binding and at H3K9me2, which is generally considered a repressive mark (Cloos et al. 2008; Kouzarides 2007). To assess Myc and FOXO3a occupancy on FOXO3a-targets (PUMA and GADD45) we carried out qChIP analysis in growing RAT-MycER cells (Gr), serum deprived for 2 days (0') and treated for 60' and 240' with OHT/serum. Thus, we determined that the PUMA E-boxII has the highest affinity for Myc binding and that Myc is recruited on this site around 60' after induction (Figure 3). The starvation of cells leads to recruitment of FOXO3a to to the fork head responsive element (FHRE) sequence and associated expression of PUMA (Figure. 1A, 1B and 4A). As soon as Myc is recruited onto the E-boxII, FOXO3a disappears from PUMA chromatin. Similar results were obtained by exploring GADD45a FHRE and TSS for FOXO3a and Myc occupancy (Figure 4B). These results indicate that upon cell cycle re-entry and Myc activation, there is a concomitant switch in promoter occupancy from FOXO3a to Myc resulting in transcriptional repression. Accordingly, we also determined that the Rbp1, large subunit of RNAPII, occupancy at the transcription start sites of both PUMA and GADD45a is sharply reduced 60' after Myc activation (Figure 4C). To work out the relevance of serum on the reciprocal inhibition of binding to the chromatin of Myc and FOXO3a we performed a qChIP analysis in the RAT-Myc$^{-/-}$ cells of FOXO3a occupancy in starved and serum-induced cells. As shown in Figure 3D, FOXO3a occupancy of the PUMA and GADD45a FHRE chromatin after 60' and 240' is marginally affected by serum addition compared to the strong reduction of FOXO3a observed in the presence of Myc, pointing at a causative role of Myc in the repression of FOXO3a-dependent transcription.

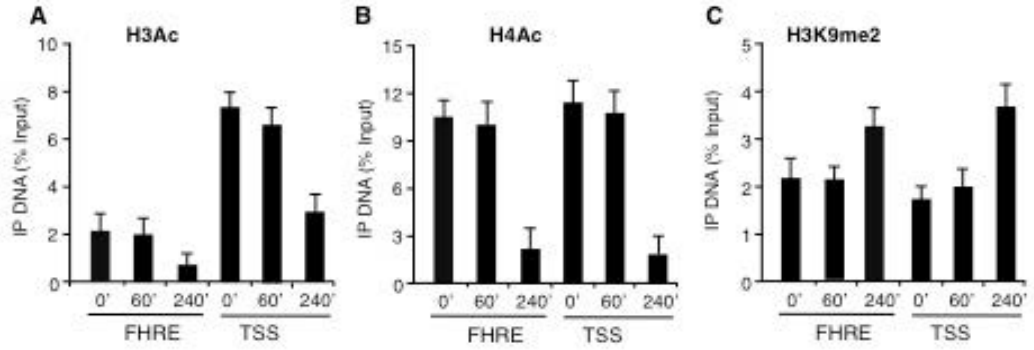

Figure 3. Myc recruitment on PUMA chromatin following Myc induction.
Myc occupancy is analyzed by qChIP in RAT-MycER serum starved cells (0') and after Myc activation (OHT/serum) a the indicate times (60' and 240'). Amplicons used for the analysis of three prutative E-boxes (-1000, +666, +1350) are shown below the simplified structure of the PUMA gene.

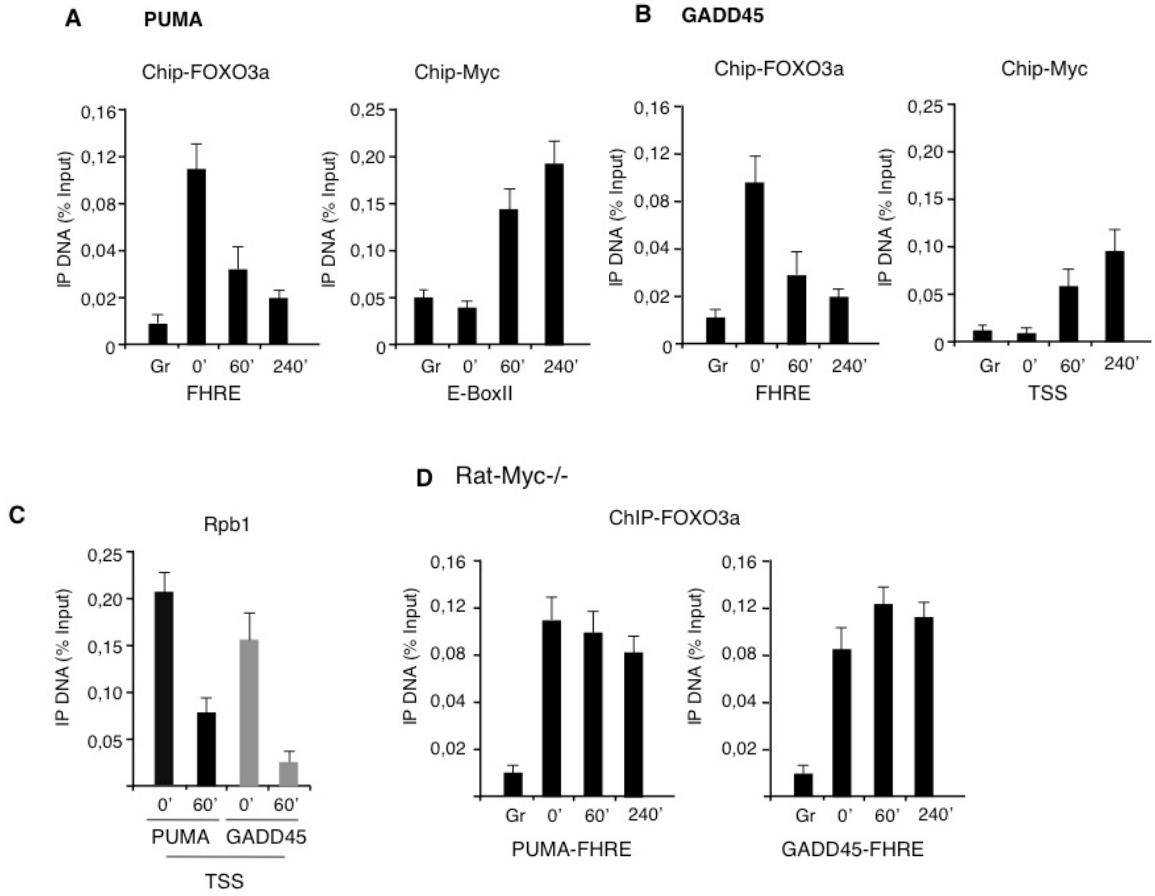

Figure 4. **Myc, FOXO3a and Rpb1 occupancy on PUMA and GADD45a chromatin.** Asynchronous RAT-MycER growing cells (Gr) were serum deprived for 2 days (0') and then treated with serum and OHT serum for Myc activation at the indicated times (30', 60' and 240'). qChIP was performed using antibodies recognizing FOXO3a (**A**), Myc (**B**) and Rpb1 (**C**). (**D**) FOXO3a occupancy on PUMA and GADD45a chromatin in growing (Gr) starved (0') and serum treated (60' and 24'0) RAT Myc-/- cells. ChIP-enriched DNA was quantified by real-time PCR analysis using amplicons reported in Supplementary Data. The values reported were calculated as fold percentage of amount of immunoprecipitated DNA relative to that present in total input chromatin. All qChIP data are presented as mean of at least three independent biological experiments each analyzed by triplicate +/- SDs. ACHR promoter amplicon was used as negative control in all experiments.

4.1.3 Myc induces H3K9 methylation and H3K4 de-acetylation on FOXO3a-targets chromatin

Myc responsive regions within the genome are characterized by specific histones marks (Guccione et al. 2006; Martinato et al. 2008; Zeller et al. 2006). High affinity Myc binding sites are marked by tri-methylation of lysine 4 in the histone H3 tail. Upon Myc binding, changes in the methylation and acetylation levels of histones H3 and H4 have been correlated to the Myc positive or negative effects on transcription efficiency of its targets (Cowling and Cole 2006; Eilers and Eisenman 2008). We analyzed by ChIP histone methylation and acetylation marks on PUMA TSS and E-boxII sequences (Figure 5) and on GADD45a FHRE and TSS sequences (Figure 6) following Myc binding, concentrating on the methylation profile of lysine 4 and 9 of histone H3 and on pan-acetylation of histones H3 and H4. While H3K4me3, H3K4me2 and H3K9me3 levels remained largely un-changed, a robust increase of H3K9me2 was found on PUMA TSS and E-boxII upon treatment with serum and MycER nuclear translocation by OHT treatment (Figure 5). Concurrent with Myc binding, we also detected a reduction in acetylated H3 and H4 levels on PUMA TSS and E-boxII sequences (Figure 5). Similar changes in chromatin modifications were found on the chromatin of the GADD45a gene (Figure 6). However, the combined treatment of RAT-MycER cells with OHT and serum does not allow for the discrimination between the effects of Myc activation and serum-induced inactivation of FOXO3a. To define the relative contribution of Myc activation and serum, we performed qChIP on RAT1 cells that only express the endogenous Myc analyzing histone modifications on GADD45a and PUMA chromatin in serum starved versus serum-treated cells. Comparing the ChIP data from RAT-MycER (Figures 5 and 6) with RAT1 cells (Figure 7 and 8) we found, as consequence of serum addiction to starved cells, a slower (4h versus 1h) reduction of acetylated H3/H4 (Figure 8 panel A and B) on both PUMA and GADD45a chromatin (Figure 7), and increased levels of methylation of H3K9 (Figure 8C) in the RAT1 cells. Furthermore, to support the relevant role of the endogenous Myc, we silenced its expression in RAT1 cells and, as shown in Figure 8D, found that the levels of H3 and H4 acetylation are chiefly unaffected in silenced cells, suggesting a causative role of Myc in the H3/H4 acetylation reduction following serum stimulation. To further support the role of Myc in the loss of H3 and H4 acetylation, we have used RAT-Myc$^{-/-}$ cells to analyze AcH3/H4 presence within FOXO3a-targets. In this Myc null cell line, after 60' and 240' of serum starvation, acetylation levels H3/H4 of the both PUMA and GADD45a chromatin is unaffected, consistent with a relevant role of Myc in the reduction of H3- and H4-acetylated levels of both PUMA and GADD45a (Figure 9A). Finally, the inhibition of histone deacetylases by TSA severely impairs Myc inhibitory effect on PUMA and GADD45a expression, following Myc induction (Figure 9B and C). These data indicate that Myc binding on PUMA and GADD45a

regulatory regions correlates with increased methylation of H3K9 and with deacetylation of H3/H4.

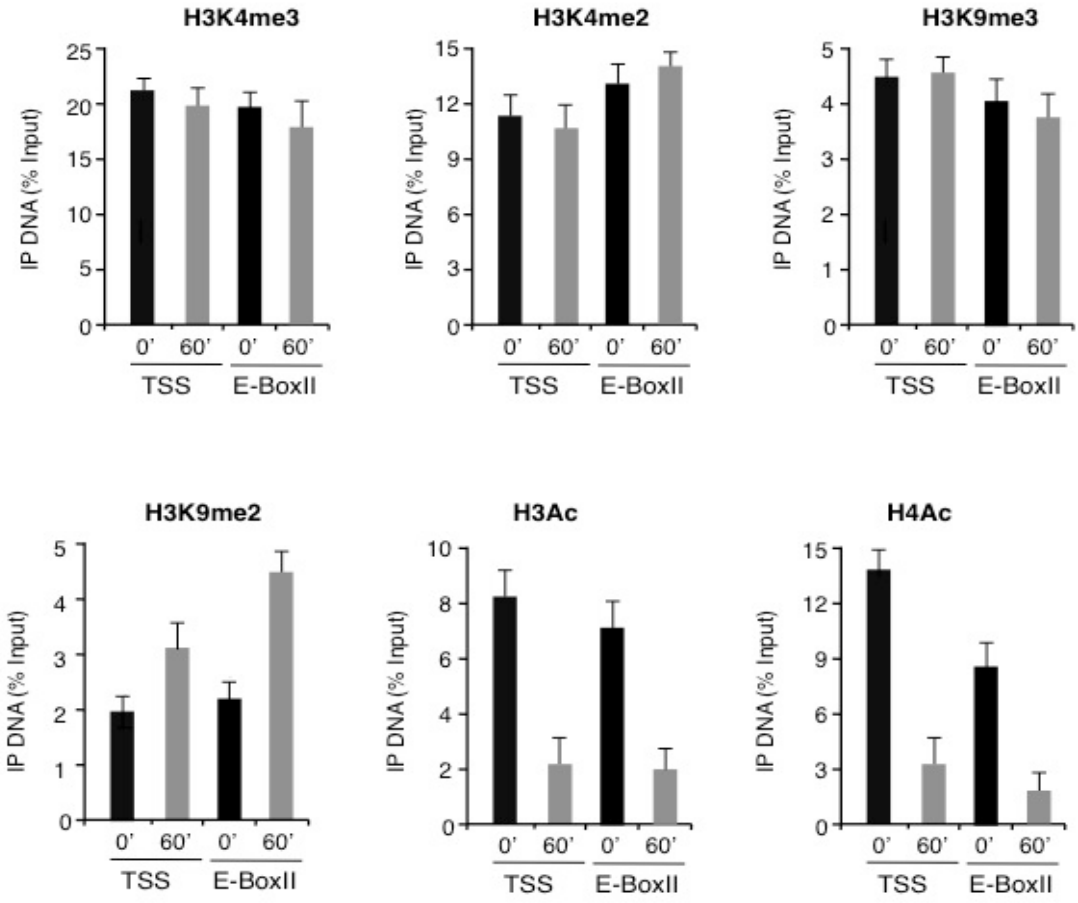

Figure 5. **Histone modifications on PUMA chromatin following Myc activation.** RAT-MycER serum starved cells (0') are compared to cells induced with OHT and serum for Myc activation (60'). qChIP was performed using specific antibodies recognizing H3K4me3, H3K4me2, H3K9me3, H3K9me2, Ac-H3 and Ac-H4 as indicated. ChIP-enriched DNA was quantified by real-time PCR analysis using amplicons surrounding PUMA transcription start site (TSS) and E-BoxII. The qChIP data are presented as in Figure 4 and ChIP-enriched DNA was quantified as previously indicated.

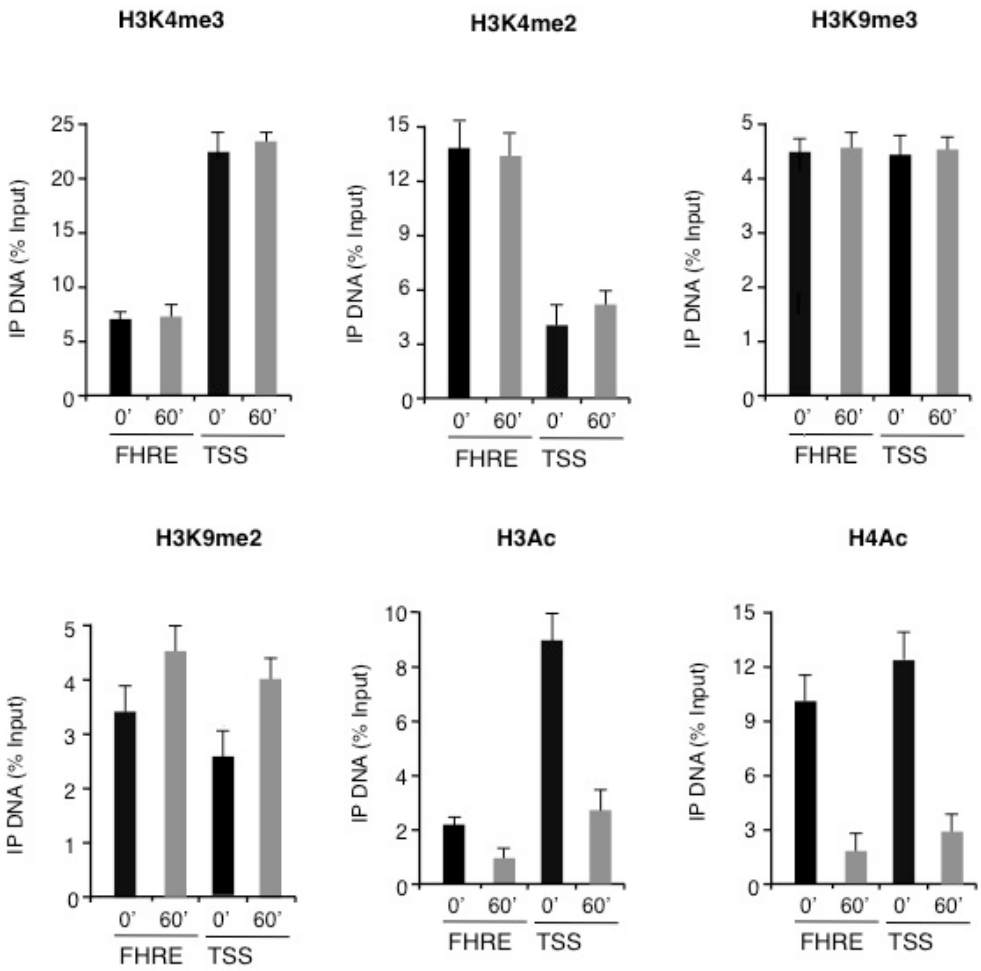

Figure 6. Histone modifications on GADD45a chromatin following Myc activation. RAT-MycER serum starved cells (00) are compared to cells induced with OHT and serum for Myc activation (60'). qChIP was performed using specific antibodies recognizing H3K4me3, H3K4me2, H3K9me3, H3K9me2, AcH3 and AcH4 as indicated. ChIP-enriched DNA was quantified by real-time PCR analysis using amplicons surrounding the TSS (-332) and FHRE (+23). The qChIP data are presented as described in Figure 4.

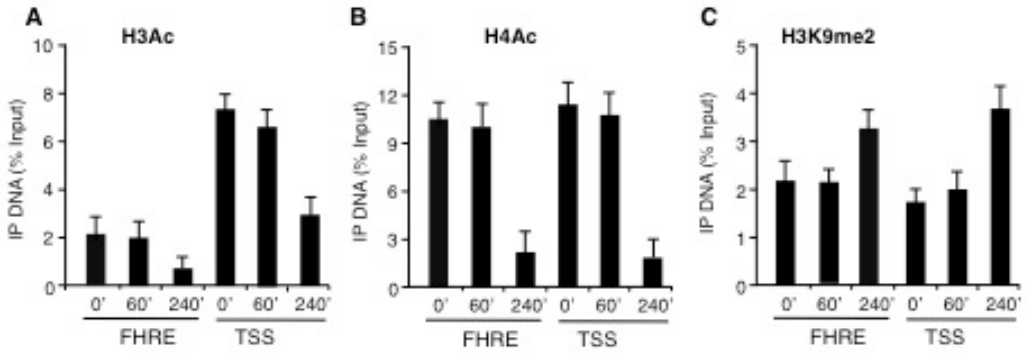

Figure 7. Myc is required for histone modification of GADD45a chromatin. Asynchronous Rat1 growing cells were serum deprived for two days (0') and then treated with serum (10%) and samples collected at the indicated times (30', 60', 240') and q ChIP was performed using specific antibodies recognizing H3Ac. H4Ac and H3K9me2, as indicated in panels A, B and C respectly. ChIP-enriched DNA was quantified by real-time PCR analysis using amplicons surrounding FHRE and TSS of GADD45a sequences.

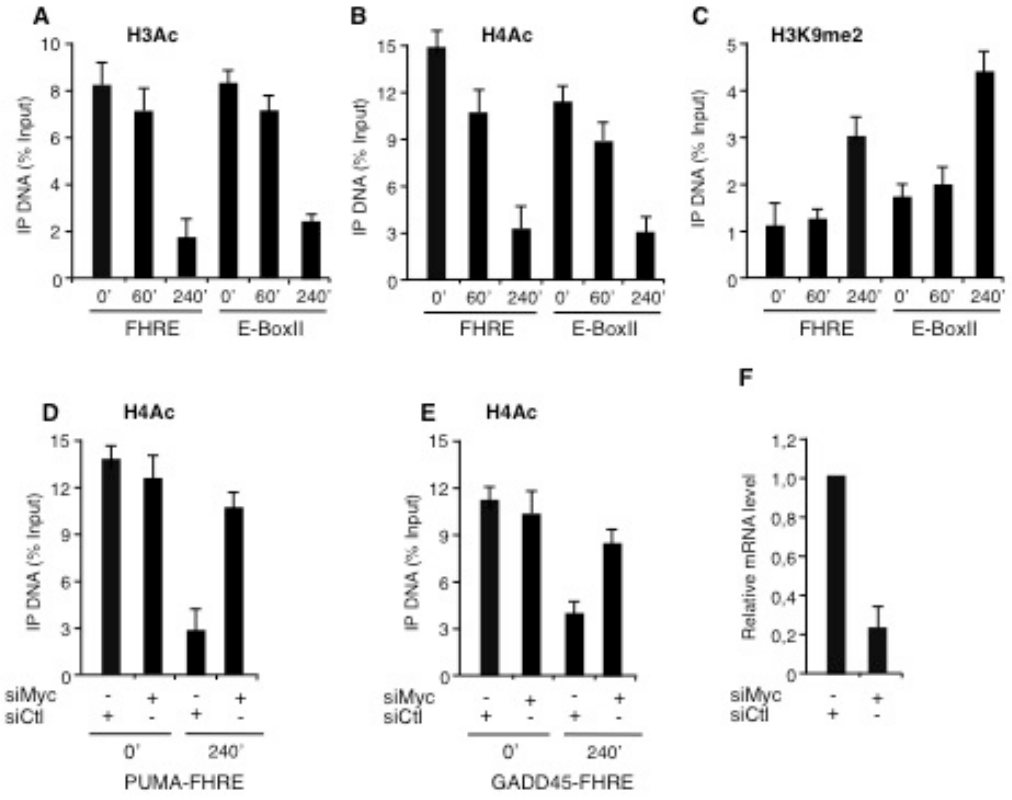

Figure 8. Myc is required for histone modification of PUMA chromatin. Asynchronous RAT1 growing cells were serum-deprived for 2 days (0') and then treated with serum (10%) and samples collected at the indicated times (30', 60' and 240') and qChIP was performed using specific antibodies recognizing H3Ac, H4Ac and H3K9me2, as indicated in panels **A**, **B** and **C**. ChIP-enriched DNA was quantified by real-time PCR analysis using amplicons surrounding PUMA, TSS and E-BoxII. The qChIP data are presented as in Figure 4. (**D** and **E**) Serum deprived (2 days) RAT1 cells (0) were treated with serum (10%) for 4h. Myc expression was inhibited with specific siRNA (siMyc) and siRNA non-targeting (siCtl) was used as scrambled RNAs. qChIP was performed using antibody recognizing H4Ac, and ChIP-enriched DNA was quantified by real-time PCR analysis using amplicons surrounding PUMA and GADD45a TSS as indicated. Error bars indicate +/- SD (n = 3). The efficiency of Myc silencing by siRNA treatments measured by qRT–PCR is shown in (F).

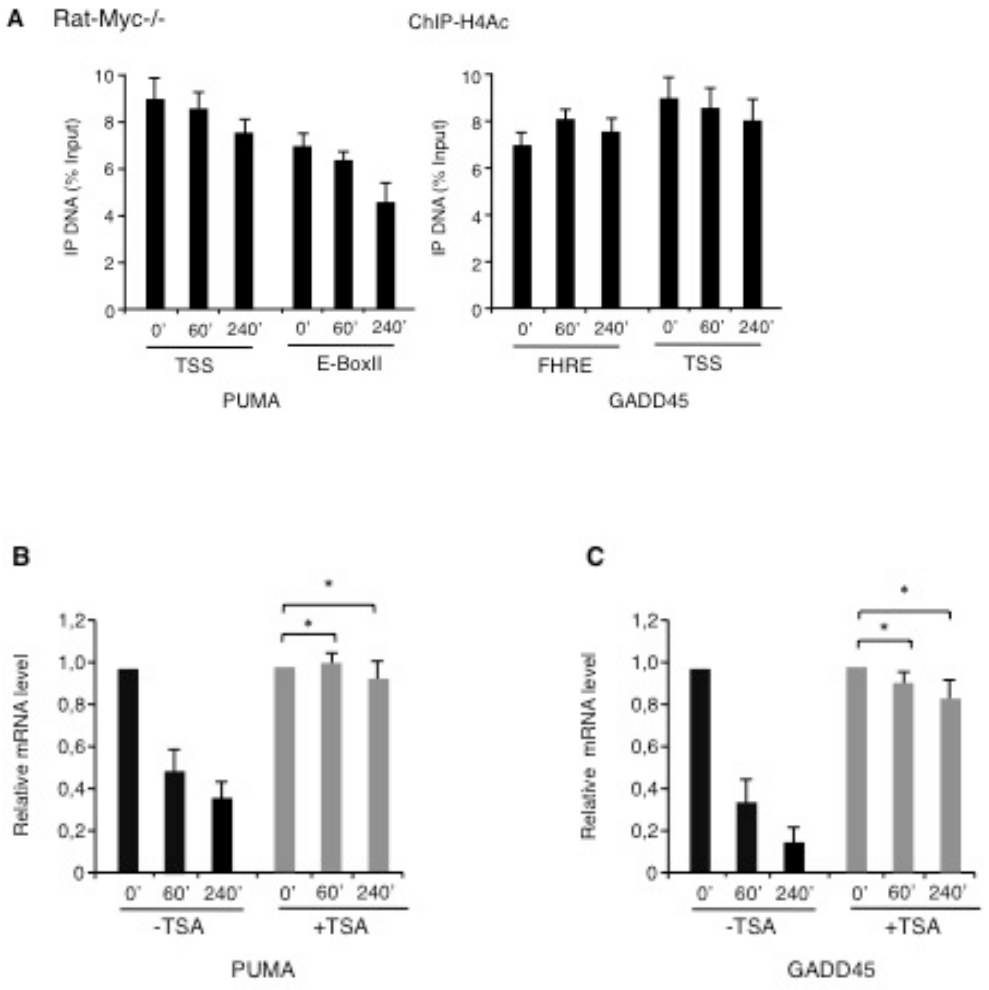

Figure 9. Histone H4 acetylation levels at Myc targets. (**A**) qChIP was performed using specific antibodies recognizing H4Ac in RAT-Myc-/- starved cells (0') and treated with OHT and serum at the indicated times (60', 240'). ChIP-enriched DNA was quantified as previously indicated. TSA impairs Myc inhibitory effect on PUMA (**B**) and GADD45a (**C**) activated transcription. Serum-deprived RAT-MycER cells (0) were treated for 600 and 2400 with OHT + serum in presence or absence of TSA (0.2 mg/ml) as indicated. PUMA and GADD45 expression levels were quantified by qRT– PCR. Error bars indicate +/- SD (n=3), *P<0.01.

4.1.4 Myc does not interfere with p53 mediated activation of PUMA

We sought to determine the specificity of Myc repressive effect on PUMA transcription independently from FOXO3a activation. PUMA expression following DNA damage is stimulated by p53 binding, through consensus p53-responsive elements located within its promoter. To determine whether Myc may suppress p53-mediated activation of PUMA, we analyzed the effect of Myc in the presence of active p53. p53 is activated by the DNA damaging compound Camptothecin (CPT) or by Nutlin-3, which disrupting the p53-MDM2 interaction thus releasing the active form of p53 (Vassilev et al. 2004). Asynchronous RAT-MycER growing cells were treated with CPT or Nutlin-3 for 4 h prior to Myc activation and PUMA mRNA levels were quantified by qRT-PCR (Figure 10A). Both CPT and Nutlin-3 treatment activate PUMA expression in the presence or absence of Myc. Moreover, we performed qChIP to analyze the occupancy of Myc and Rpb1 on PUMA regulatory regions following p53 activation. Figure 10B shows that, in condition in which CPT and Nutlin-3 activate PUMA, E-box occupancy by Myc is unaffected. Accordingly, TSS occupancy by Rpb1 in cells with active p53 remains unchanged after Myc activation (Figure 10C). These data demonstrate that Myc binding does not interfere with p53-mediated activation of PUMA and indicate that Myc is not a global repressor of PUMA expression.

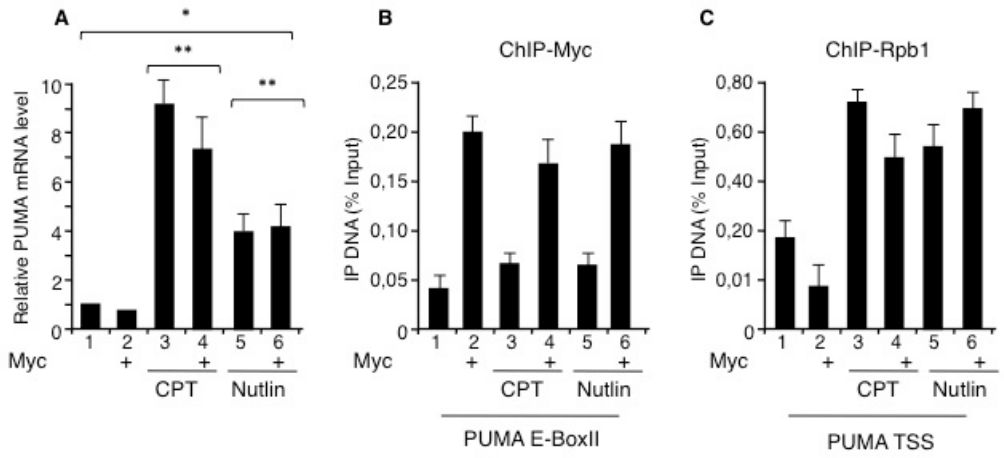

Figure 10. Myc does not repress p53-dependent PUMA activation. (**A**) Growing RAT-MycER cells were treated with OHT for Myc induction (Myc) for 4h. OHT-treated and control-untreated cells were incubated with CPT (12mM for 4h) or Nutlin-3 (10mM for 4h) and then PUMA mRNA levels were quantified by qPCR as described in Figure 1. In parallel, recruitment of Myc (**B**) and Rpb1(**C**) on PUMA chromatin was determined by qChIP using the E-BoxII and TTS amplicons. All qChIP data are presented as mean of at least three independent biological experiments each analyzed by triplicate SDs, *P<0.05, **P<0.01. (**D**) Schematic model underlying the reciprocal role of Myc and FOXO3a in regulation of expression of growth promoting and growth arresting genes.

4.2. SUMO-activating SAE1 transcription is positively regulated by Myc

Our previous results have shown that the proapoptotic PUMA gene is a Myc target and through recruitment to an E-box binding site on its promoter, Myc cooperates with the PI3/AKT pathway to repress FOXO3a mediated activation of PUMA expression (Amente et al. 2010).
During that study we were intrigued by the presence of a Myc responsive RNAPII peak in the second intron of PUMA locus in condition in which PUMA expression was inhibited. This finding instigated a search of actively expressed genes responsive to Myc activation in the region downstream of PUMA resulting in the identification of SUMO-activating enzyme SAE1 gene whose transcription proceeds in the opposite strand to PUMA. SAE1 in association with SAE2 form a critical component of the SUMO-activating enzyme necessary for SUMO conjugation to proteins (Hay 2005).To determine the expression of SAE1 in the presence of hyper-activated Myc protein, we used the RAT-MycER and the human retinal hT-RPE-MycER cell lines in which the inducible Myc estrogen receptor fusion transgene is activated upon treatment with tamoxifen (Alfano et al. 2010; Amente et al. 2011). As shown in figure 11A, in RAT-MycER, SAE1 expression as well as NUC, a known Myc target, increases in response to Myc activation while the levels of expression of PUMA are inhibited. To determine the contribution of Myc to the SAE1 activation we silenced Myc in the RAT-MycER cells and found abrogation of SAE1 transcription (Figure 11B). To further determine the contribution of Myc to SAE1 activation, we used the isogenic RAT-Myc$^{-/-}$ cells and measured SAE1 expression levels in starved versus serum-induced cells. As shown in figure 11C, SAE1 expression slightly increased upon serum addition while the expression was significantly higher upon transfection of Myc into RAT-Myc$^{-/-}$ cells. Collectively these results suggest that SAE1 expression is indeed regulated by Myc. In this respect we analyzed SAE1 expression in the retinal human Myc inducible cell line hT-RPE-MycER and, as shown in figure 12A, Myc activation results in induction of SAE1 expression at levels comparable to NUC. To explore the role of Myc in SAE1 activation we scanned its genomic sequences for putative Myc binding sites. Several E-box were found (Figure 12B), and we focalized our attention on two closely associated E-box in position close to the TSS site (-170 and -101). Most importantly these E-boxes are located in a region with high level of H3K4me3, a prerequisite for Myc binding (Figure 12B) (Guccione et al. 2006, Martinato et al. 2008). To assess Myc occupancy on SAE1 we carried out qChIP on the hT-RPE-MycER cells, which were growth factors-deprived for 2 days (0) and treated for 6 hrs with OHT for Myc activation. Chromatin immunoprecipitated using an anti-Myc antibody was analyzed using amplicons spanning the SAE1 and NUC E-boxes and the qChIP data (Figure 12B) showed that Myc is recruited on the E-box sites at the SAE1 promoter with efficiency comparable to recruitment on NUC.

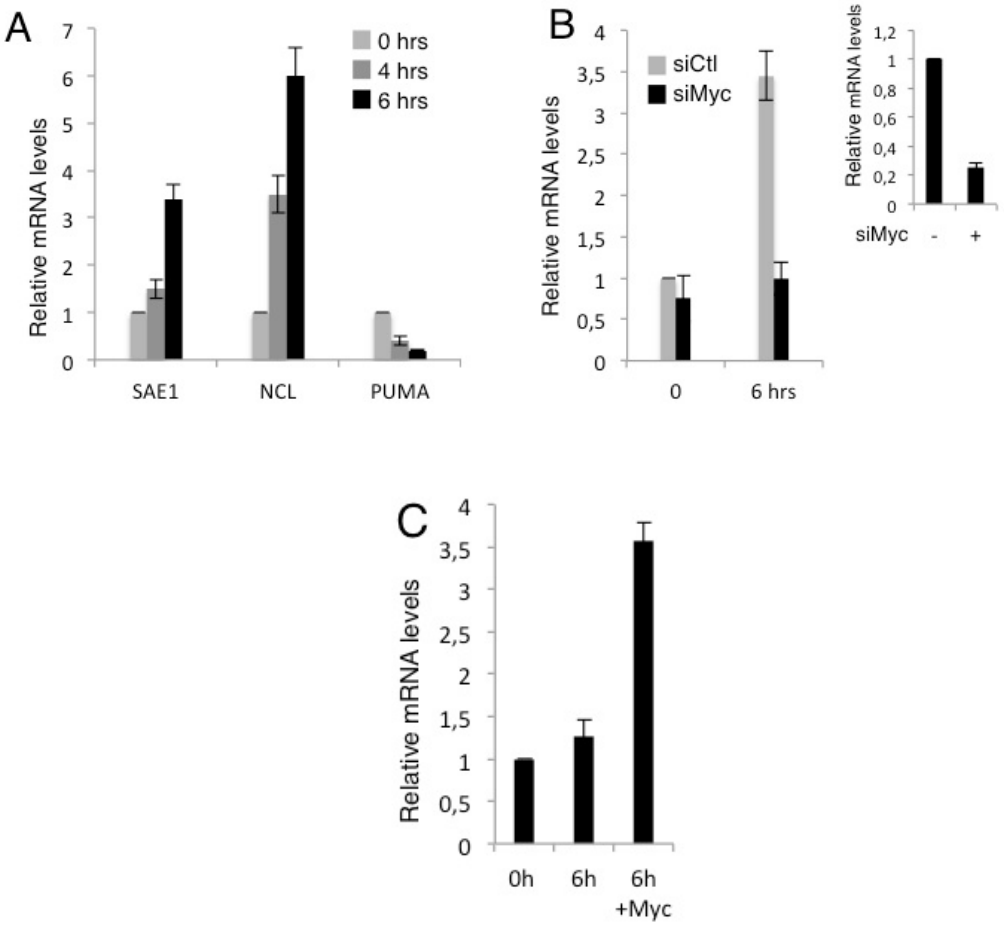

Figure 11. Myc activates SAE1 expression. (**A**) mRNA expression levels of SAE1, NUC and PUMA were quantified by qRT –PCR in quiescent cells (0) and after 4 and 6hrs of treatment with serum and OHT. (**B**) Myc expression was inhibited with specific siRNA (siMyc) and siRNA non-targeting (siCtl) was used as scrambled RNAs. SAE1 mRNAs expression levels were quantified by qRT–PCR in quiescent cells (0) and 6hrs of treatment with serum and OHT. The efficiency of Myc silencing by siRNA treatments measured by qRT–PCR is shown on the right. (**C**) RAT-Myc-/- cells as well as cells transfected with a Myc expression vector were serum deprived for 48 hrs. SAE1 mRNA levels were evaluated by qRT– PCR 6 hrs after serum induction. Values were compared to quiescent cells (0).

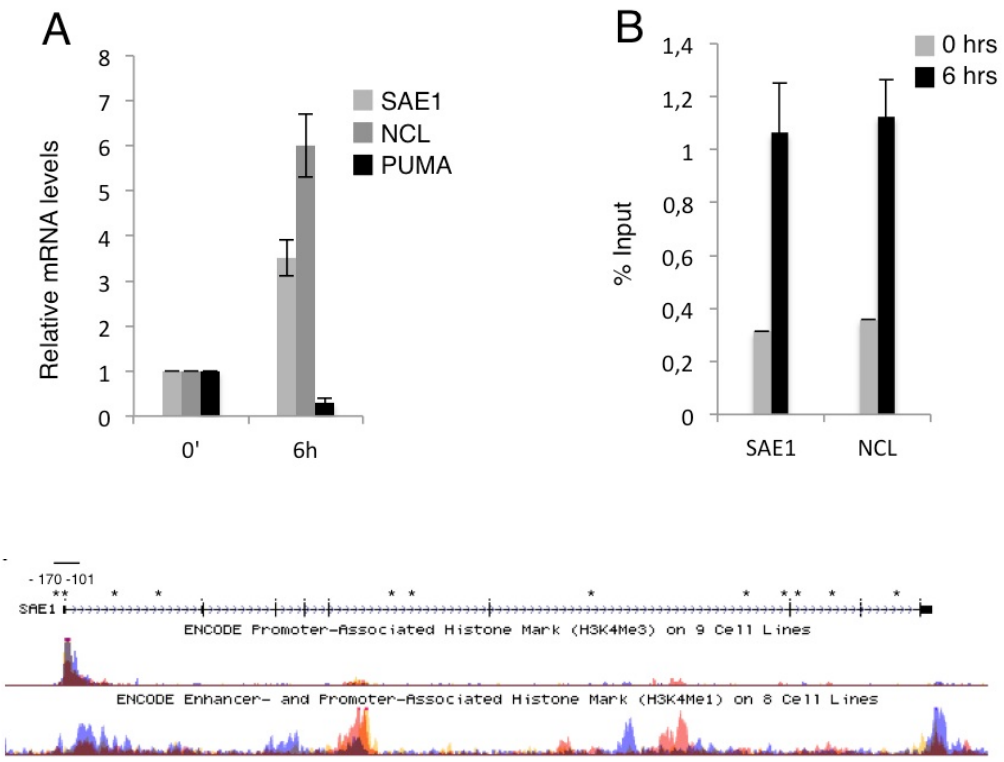

Figure 12. (**A**) hT-RPE-MycER cells were synchronized by 2 days of growth factors deprivation. SAE1, NUC and PUMA mRNAs expression levels were quantified by qRT–PCR in synchronized (0) and cells treated with growth factor + OHT (6hrs). All mRNA levels were normalized to β-glucuronidase (GUS) mRNA levels and all values represent the average of at least three independent experiments. Error bars indicate SD. Protein expression is shown in immunoblots of whole-cell extracts with anti-SAE1 and actin for loading control. (**B**) An adapted UCSC genome browser view of SAE1 genomic sequence displaying H3K4me3 and H3K4me1 levels and putative E-box (asterisks). Myc occupancy on SAE1 and NUC chromatin in synchronized (0) and Myc induced hT-RPE-MycER cells for 6hrs is shown. ChIP-enriched DNA was quantified by real-time PCR analysis using amplicon covering the region containing the Myc binding E-boxes as shown in Figure 12A.

4.3 PUMA and SAE1: two Myc targets in mouse mammary cells

In addition to the role in cancer, Myc is important for the transcriptional regulation in embryonic stem (ES) cells and somatic cell reprogramming. Indeed, Myc overexpression in adult cells can block differentiation and cooperates with *Oct*3/4, Sox2 and Klf4 in the reprogramming of adult differentiated cells into induced pluripotent stem cells (iPS) (Takahashi and Yamanaka, 2006). Myc is able to reprogram mouse mammary progenitor cells into mammary stem cells, as Myc expressing primary mammary cells acquire the ability to form mammospheres (Pasi et al. 2011). Recently, the identification of genes vital to support Myc-addicted tumors through a genome wide genetic screen for Myc-synthetic lethal (MySL) shRNAs in human mammary epithelial cells has been reported (Evan 2012; Kessler et al. 2012). SAE1 and SAE2 genes are the most significant candidates that have been isolated in this study (Kessler et al. 2012). The SAE1/2 ‘s loss induces mitotic catastrophe and cell death upon Myc hyper-activation in cancer cells (Kessler et al. 2012). This latter finding (Kessler et al. 2012) prompted us to determine if Myc is able to regulate PUMA and SAE1 transcription also in Myc expressing primary murine mammary cells, and if these genes can exert a similar or different role in the Myc-driven cell reprogramming. To investigate this, we cultured primary cells from wild-type (WT) mammary tissue in non-adherent conditions, which allow cells to proliferate in suspension as floating colonies (mammospheres) (Dontu et al. 2003). Their preliminary characterization revealed that, as reported, WT mammospheres derive from the clonal expansion of single cells endowed with self-renewal potential, are composed of epithelial cells, and are enriched in multipotent cells capable of differentiating along different lineages (Cicalese et al. 2009). To determine the expression of SAE1 and PUMA in the presence of hyper-activated Myc protein, we performed experiments infecting primary mammary cells with either lentivirus expressing MycER or its empty vector control. Control virus-infected mammospheres prepared from wilt-type mice could be maintained only for a few passages in tissue culture, suggesting exhaustion of stem cell population. In contrast, mammospheres infected with the virus-expressing MycER could be easily expanded with no signs of crisis or stem cell exhaustion. The reprogramming of mammary progenitor cells into mammary stem cells was performed in the presence of 4-hydroxytamoxifen (0, 4, 8, 24, 30hrs) to increase the nuclear MycER protein levels. Thus, we analyzed PUMA and SAE1 expression in mammospheres in response to Myc activation. As shown in figure 13 panel A and B, in mammospheres, SAE1 expression as well as NUC and CAD, known Myc targets, increased in response to Myc activation after 8hrs of OHT treatment, in correspondence to the peak of the Myc expression levels, while at the same time point the levels of expression of PUMA are inhibited as previously described in RAT-MycER and in hT-RPE-MycER cells. As previously described, PUMA activation is dependent by a functional p53 and mediated by a p53-responsive element in its promoter.

Indeed, to address the Myc-mediated regulation of PUMA, we analyzed either the expression of common Myc and p53-targets genes (p21 and GADD45a) and only p53-targets (BAX and NOXA) (Figure 14). The activation of p53 protein is evident at later time points of Myc induction, highlighting the p53-dependent regulation of Myc during the self-renewal in normal stem cells. Collectively, these data determined that the expression of SAE1 and PUMA depends on Myc activity. In particular, we have established that SAE1 and PUMA expression is always inversely correlated.

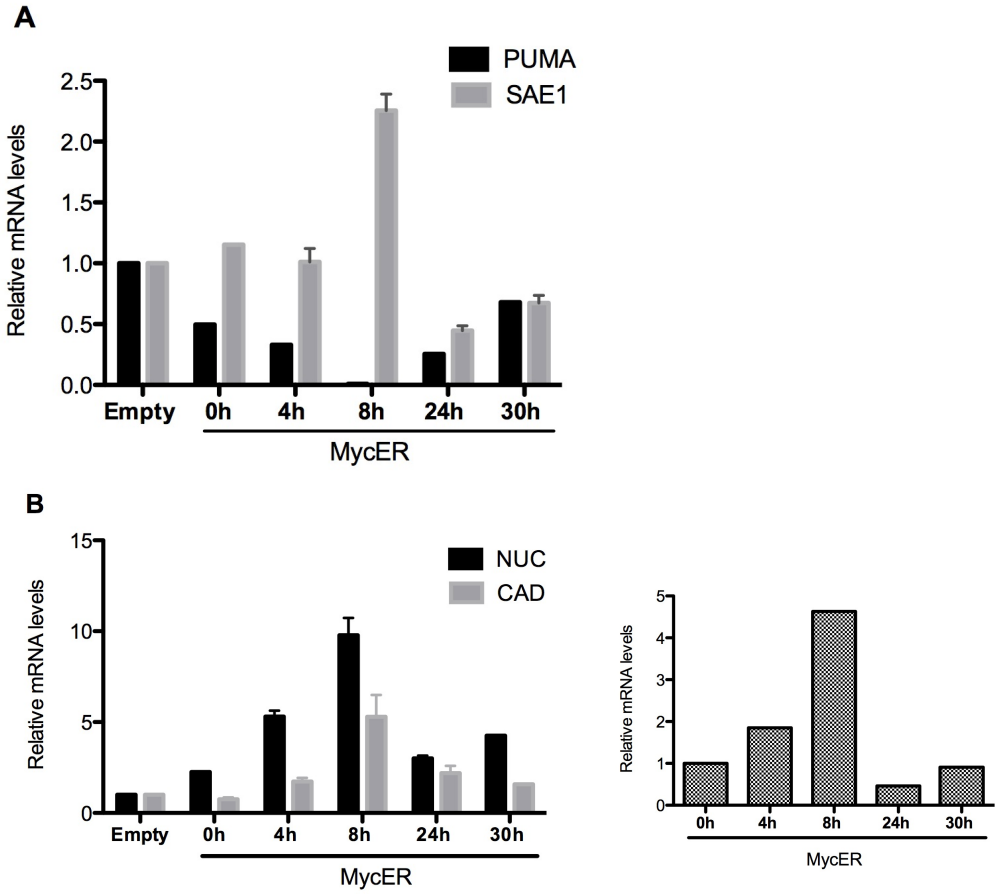

Figure 13. Myc regulates PUMA and SAE1 expression. (**A**) mRNA expression levels of PUMA and SAE1, were quantified by qRT –PCR in wt mammospheres infected with empty vector and MycER lentivirus (0h) and after 4, 8, 24, 30 hrs of treatment with OHT. (**B**) Myc targets expression NUC and CAD were measured in wt mammospheres infected with MycER lentivirus and then treated or not (0h) with OHT (4, 8, 24, and 30 hrs); Myc expression was measured by qRT–PCR using with specific hMyc oligos. Values were compared to empty vector infecting mammospheres.

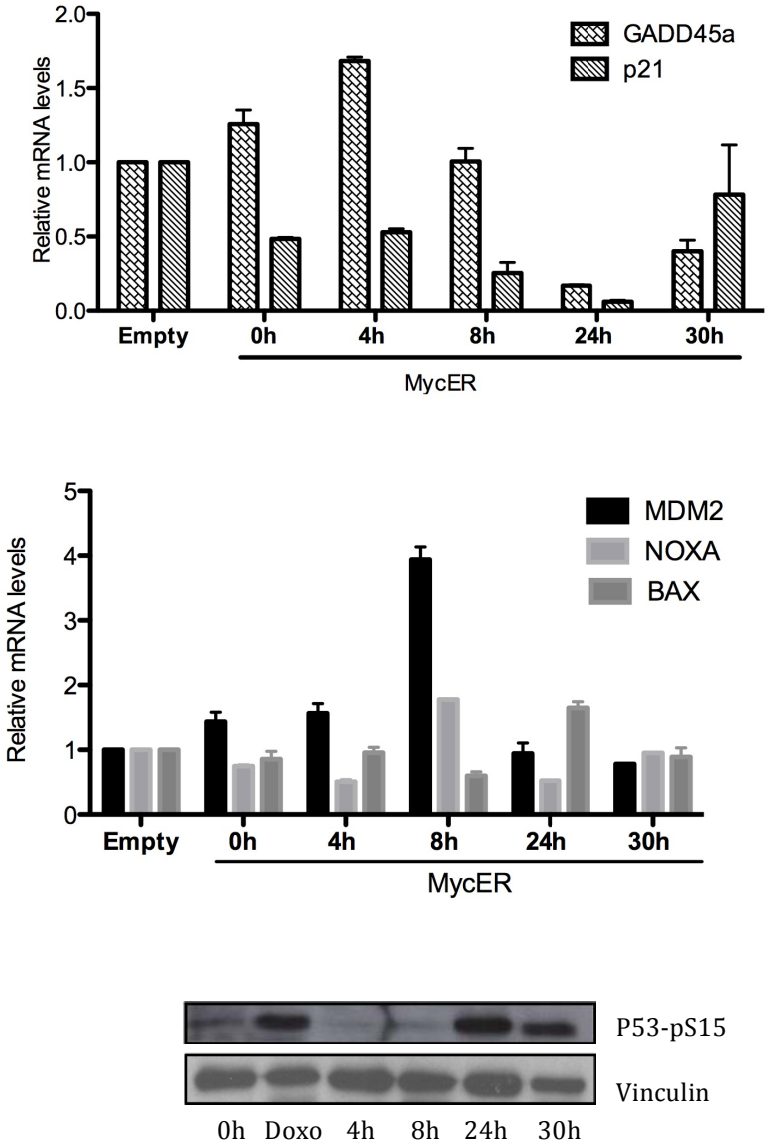

Figure 14. The expression profile obtained demonstrates that p53 pathway is activated after 24hrs of OHT treatment in mammospheres infected with MycER vector; mRNA expression levels of GADD45a and p21 were quantified by qRT–PCR in wt mammospheres infected with empty vector or MycER lentivirus (0h) and after 4, 8, 24, 30hrs of treatment with OHT. MDM2 displays a peak of expression at 8h, whereas NOXA and BAX show little variation in levels of expression in respect to cells not treated with OHT. The maximum phosphorylation level of of serine 15 of p53 that corresponds to the active form of p53 was seen at 24h.

4.3.1 PUMA and SAE1 expression after reprogramming of homogeneous mouse mammary cells into stem cells mediated by Myc

Since SAE1 protein seems to play ad important role in the Myc-synthetic lethal (MySL) phenotype observed using shRNAs in human mammary epithelial cells, as reported by Kessler et al. (2012), it appeared intriguing to study the expression of these Myc targets in homogeneous population of mammary progenitor cells, obtained using a previously described with a PKH26-based label-retaining protocol (Figure 15). The primary mammary cells were pulse-labeled with PKH26 and then cultured as mammospheres for one passage, followed by flowsorting of PKH26-high cells (about 1.07 % of all cells, representing stem cells) and PKH26-negative cells (about 70% of all cells, representing progenitor cells) (Figure 15A). The PKH26-negative cells were then infected with a control lentivirus or a lentivirus-expressing MycER (Littlewood et al. 1995). Five thousand infected cells were cultured under non-adherent conditions to generate mammospheres, which were then passaged on a weekly basis. The control infected progenitor cells formed mammospheres with very low efficiency even at the first passage and both the mammospheres number and the cumulative cell number declined to practically zero within a few passages (Figure 16C). In contrast, the MycER-expressing progenitor cells were reprogrammed into mammary stem cells, as determined by their ability to form mammospheres (Figure 16B). Unexpectedly, PUMA expression was upregulated in the presence of MycER, while SAE1 expression was unchanged (Figure 16D). As shown in figure 16, in mammospheres, PUMA expression as well as the known NUC and CAD genes, increase in response to Myc activation. The PUMA activation can be caused by p53-activation, indeed, p53 targets (p21 and BAX) are upregulated in response to Myc activation (Panel F and G).

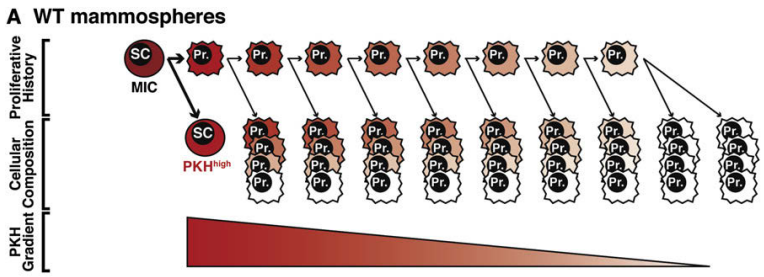

Figure 15. Modeled Kinetics of stem cell devisions within Normal Mammospheres The model represents the kinetics of cell divisions during the clonal expansion of one normal mammosphere-initiating cell (MIC). The scheme reports the proliferative history of one of mammosphere initating cell (upper part), the projected cellular composition of the formed mammospheres (middle part), and the progressive decrease of PKH fluorescence intensity (PKH gradient) (Cicalese et al. 2009).

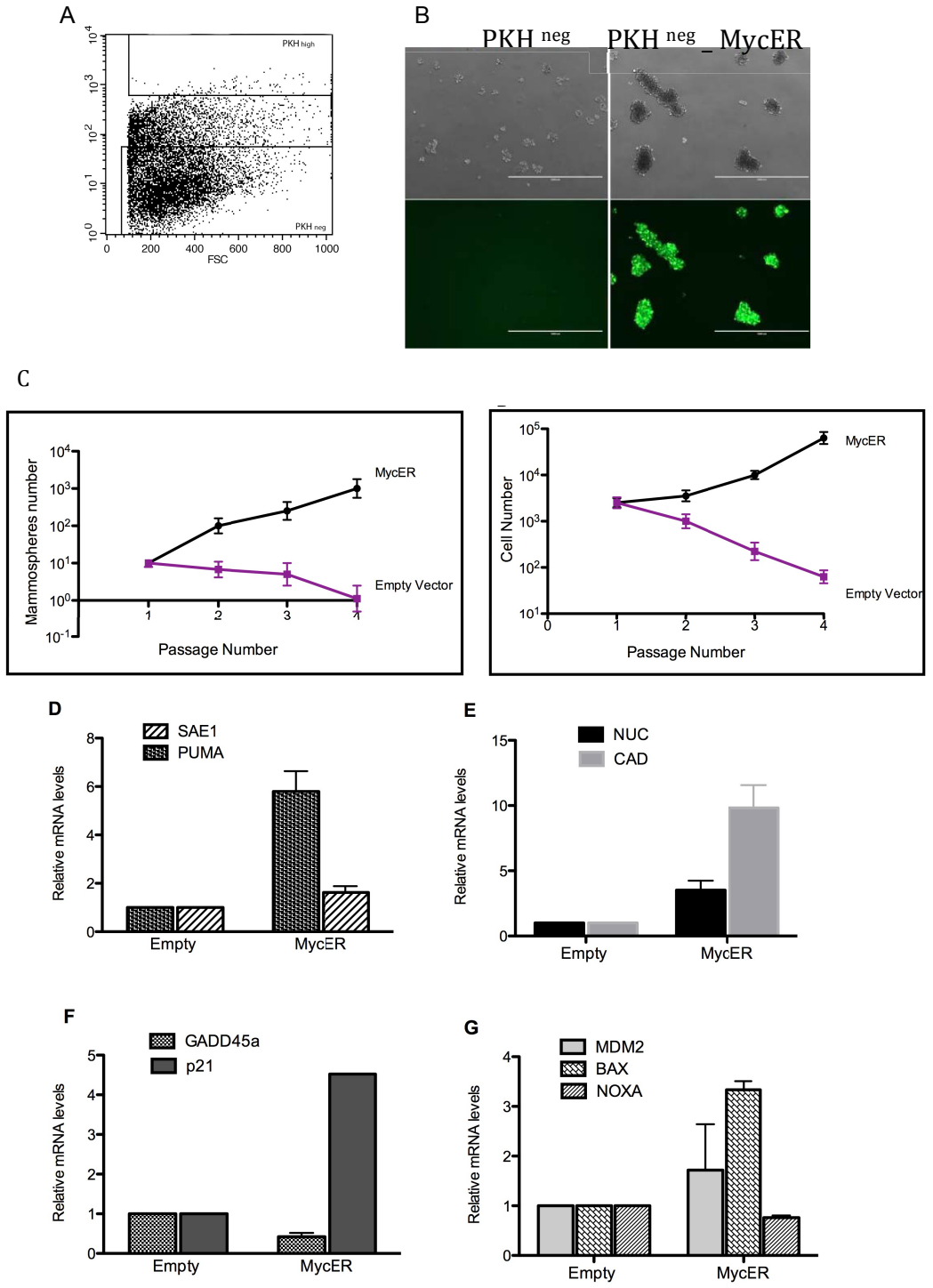

Figure 16. Reprogramming of progenitor mammary cells to stem cells by MycER (A and B) FACS distribution of PKH ^{high}, PKH ^{low}, and PKH ^{neg} cells and image of M3 mammospheres obtained after replating and infection with MycER–lentivirus of PKH ^{neg} cells. **(C)** PKH26-negative cells, which are devoid of stem cells, were isolated from secondary mammospheres and infected with a lentivirus-expressing MycER or with a control virus (Empty vector). The cells were cultured under non-adherent conditions and mammospheres number and cumulative cell number were determined at each passage. Results are presented as means +/-SD. **(D)** PUMA and SAE1 expression was measured in wt mammospheres one week post-infection with MycER lentivirus or the corresponding empty vector. The espression profile obtained demonstrates an activation of proapoptotic p53 targets **(F and G)** and this phenotype obscured the downregulation of PUMA and upregulation of SAE1 that we expected to see, albeit we have successfully induced Myc expression and its classical downstream targets (e.g. NUC and CAD) **(E)**.

Conclusions

The abrogation of FOXO3a function promotes foci formation by Myc *in vitro*, and dramatically accelerates Myc driven lymphomagenesis *in vivo* (Bouchard et al. 2001; Bouchard et al. 2004). In this study we provide a suitable explanation for this behavior, demonstrating strong evidence for the cooperation between Myc and PI3/AKT/FOXO3a pathways in the activation of Myc targets. Our findings propose that the synergy between Myc and PI3/AKT/FOXO3a pathway has an important role not only in the activation of multiple Myc target genes involved in cell proliferation, but also in repression of FOXO3a targets involved in anti-proliferative function such as PUMA and GADD45a. Reciprocal control by Myc and FOXO3a has been also described in the regulation of p27Kip1 transcription (Chandramohan et al. 2008; Dijkers et al. 2000; Stahl et al. 2002), and it has been suggested that Myc inhibits p27 transcription via physical association with FOXO3a (Chandramohan et al. 2008). The significant overlap between FOXO3a and Myc targets includes CyclinD2, CDK4 CyclinE2 growth-promoting factors and PUMA, p27Kip1 and GADD45a growth-arrest factors. Our findings provide a mechanistic model for explaining the cooperation of Myc and PI3/AKT-signaling in repression of FOXO3a-dependent activation. Serum external growth factors induce activation of the AKT survival kinase leading to phosphorylation of FOXO3a. However, AKT activation is not fully sufficient to repress FOXO3a targets and it contributes further to repression by establishing the repressive chromatin marks characterized by deacetylation of H3/H4 histones and increased levels of H4K9me2. The inhibition of FOXO3a-mediated activation of PUMA, by aberrant expression of Myc correlates with functional relationship between PUMA and Myc. PUMA has been proposed as a tumor modifier gene that limits lymphomagenesis. Using genetically defined mice it was shown that PUMA plays a physiological role in suppressing Myc-induced murine B-cell lymphomagenesis, and PUMA deficiency alleviates Myc-induced apoptosis and accelerates Myc lymphomagenesis. The importance of the Myc-role in tumor cells is highlighted of the pervasive nature of Myc regulatory network. Indeed, recently, it has been documented that a specific pathway involving SAE1/2, a critical component of the SUMO activating enzyme genes, is required to support Myc-addicted tumors. Thus, Sae1/2 acts as Myc-synthetic lethal in Myc-driven tumors; inhibition of SAE triggers mitotic spindle defects in Myc-expressing cells, eliciting mis-segregation of chromosomes and commitment to apoptosis (Kessler et al. 2012). Our study adds news insight in this context since we show that Myc directly activates SAE1 transcription, suggesting that its oncogenic SAE1-dependent activity is ensured by Myc itself through direct binding and transcriptional activation of SAE1 expression. Thus, recruitment of Myc on SAE1 modulates its expression supporting Myc oncogenic program by activation of sumoylation-dependent Myc-switchers. Intriguing is the fact that PUMA and SAE1 are adjacent on the human chromosome 19 and that their expression has been always found

inversely correlated. While Myc cooperates with PI3/AKT pathway to repress PUMA transcription, hyper activation of Myc activates SAE1 transcription.
Since the apparent parallels between tumor cells and normal stem cells, we had a great interest in the study of the transcriptional regulation of PUMA and SAE1 during Myc driven reprogramming. Our data show that Myc is able to regulate the transcription of PUMA and SAE1 in a heterogeneous population of mouse mammary progenitor cells after reprogramming into mammary stem cells. The regulation of PUMA and SAE1 is inversely correlated as in other models utilized. In particular, PUMA is down regulated in mammospheres with high expression of Myc, whilst SAE1 is upregulated at the same condition of Myc expression. The regulation of these two Myc-targets is correlated with the profile of expression of p53 targets. Accordingly, we found no activation of the proapoptotic p53 downstream effectors.
A recent review has postulated that in normal stem cells and cancer stem cells, Myc expression alone sustains a pool of expanding stem cells in the absence of transformation or apoptosis (Verga Falzacappa et al. 2012). Indeed, Myc expression in mammary stem cells mimics the loss or attenuation of p53. On the other end, the expression profile obtained in a homogeneous population of progenitor cells (PKHneg cells) after Myc-reprogramming demonstrated an absence of inversely correlation of expression between PUMA and SAE1, albeit we have successfully induced Myc expression and its classical downstream targets (e.g. NUC and CAD). The activation of proapoptotic p53, as demonstrated by up-regulation of p21, BAX and PUMA, supports the observation that Myc is not able to interfere with p53-mediated activation of PUMA, as seen in RAT-MycER model.
Nevertheless the relevance role of Myc during reprogramming of somatic stem cells, the molecular mechanisms by which it operates is not understood and further investigations will be necessary to understand the role of these Myc targets, nonetheless it is recognized the crucial role of p53-Myc axis in regulating normal stem cell and cancer stem cell pool.

Bibliography

Alfano, D., Votta, G., Schulze, A., Downward, J., Caputi, M., Stoppelli, M.P., and Iaccarino, I. (2010). Modulation of cellular migration and survival by c-Myc through the downregulation of urokinase (uPA) and uPA receptor. Mol Cell Biol *30*, 1838-1851.

Almstrup, K., Hoei-Hansen, C.E., Wirkner, U., Blake, J., Schwager, C., Ansorge, W., Nielsen, J.E., Skakkebaek, N.E., Rajpert-De Meyts, E., and Leffers, H. (2004). Embryonic stem cell-like features of testicular carcinoma in situ revealed by genome-wide gene expression profiling. Cancer Res *64*, 4736-4743.

Amente, S., Zhang, J., Lavadera, M.L., Lania, L., Avvedimento, E.V., and Majello, B. (2011). Myc and PI3K/AKT signaling cooperatively repress FOXO3a-dependent PUMA and GADD45a gene expression. Nucleic Acids Res *39*, 9498-9507.

Berns, K., Hijmans, E.M., and Bernards, R. (1997). Repression of c-Myc responsive genes in cycling cells causes G1 arrest through reduction of cyclin E/CDK2 kinase activity. Oncogene *15*, 1347-1356.

Bouchard, C., Dittrich, O., Kiermaier, A., Dohmann, K., Menkel, A., Eilers, M., and Luscher, B. (2001). Regulation of cyclin D2 gene expression by the Myc/Max/Mad network: Myc-dependent TRRAP recruitment and histone acetylation at the cyclin D2 promoter. Genes Dev *15*, 2042-2047.

Bouchard, C., Marquardt, J., Bras, A., Medema, R.H., and Eilers, M. (2004). Myc-induced proliferation and transformation require Akt-mediated phosphorylation of FoxO proteins. Embo J *23*, 2830-2840.

Bouchard, C., Thieke, K., Maier, A., Saffrich, R., Hanley-Hyde, J., Ansorge, W., Reed, S., Sicinski, P., Bartek, J., and Eilers, M. (1999). Direct induction of cyclin D2 by Myc contributes to cell cycle progression and sequestration of p27. Embo J *18*, 5321-5333.

Chandramohan, V., Mineva, N.D., Burke, B., Jeay, S., Wu, M., Shen, J., Yang, W., Hann, S.R., and Sonenshein, G.E. (2008). c-Myc represses FOXO3a-mediated transcription of the gene encoding the p27(Kip1) cyclin dependent kinase inhibitor. J Cell Biochem *104*, 2091-2106.

Cicalese, A., Bonizzi, G., Pasi, C.E., Faretta, M., Ronzoni, S., Giulini, B., Brisken, C., Minucci, S., Di Fiore, P.P., and Pelicci, P.G. (2009). The tumor

suppressor p53 regulates polarity of self-renewing divisions in mammary stem cells. Cell *138*, 1083-1095.

Cloos, P.A., Christensen, J., Agger, K., and Helin, K. (2008). Erasing the methyl mark: histone demethylases at the center of cellular differentiation and disease. Genes Dev *22*, 1115-1140.

Coller, H.A., Grandori, C., Tamayo, P., Colbert, T., Lander, E.S., Eisenman, R.N., and Golub, T.R. (2000). Expression analysis with oligonucleotide microarrays reveals that MYC regulates genes involved in growth, cell cycle, signaling, and adhesion. Proc Natl Acad Sci U S A *97*, 3260-3265.

Cowling, V.H., and Cole, M.D. (2006). Mechanism of transcriptional activation by the Myc oncoproteins. Semin Cancer Biol *16*, 242-252.

Dijkers, P.F., Medema, R.H., Lammers, J.W., Koenderman, L., and Coffer, P.J. (2000). Expression of the pro-apoptotic Bcl-2 family member Bim is regulated by the forkhead transcription factor FKHR-L1. Curr Biol *10*, 1201-1204.

Dominguez-Sola, D., Ying, C.Y., Grandori, C., Ruggiero, L., Chen, B., Li, M., Galloway, D.A., Gu, W., Gautier, J., and Dalla-Favera, R. (2007). Non-transcriptional control of DNA replication by c-Myc. Nature *448*, 445-451.

Dontu, G., Abdallah, W.M., Foley, J.M., Jackson, K.W., Clarke, M.F., Kawamura, M.J., and Wicha, M.S. (2003). In vitro propagation and transcriptional profiling of human mammary stem/progenitor cells. Genes Dev *17*, 1253-1270.

Eilers, M. (1999). Control of cell proliferation by Myc family genes. Mol Cells *9*, 1-6.

Eilers, M., and Eisenman, R.N. (2008). Myc's broad reach. Genes Dev *22*, 2755-2766.

Evan, G. (2012). Cancer. Taking a back door to target Myc. Science *335*, 293-294.

Evan, G.I., Wyllie, A.H., Gilbert, C.S., Littlewood, T.D., Land, H., Brooks, M., Waters, C.M., Penn, L.Z., and Hancock, D.C. (1992). Induction of apoptosis in fibroblasts by c-myc protein. Cell *69*, 119-128.

Frank, S.R., Schroeder, M., Fernandez, P., Taubert, S., and Amati, B. (2001). Binding of c-Myc to chromatin mediates mitogen-induced acetylation of histone H4 and gene activation. Genes Dev *15*, 2069-2082.

Garrison, S.P., Jeffers, J.R., Yang, C., Nilsson, J.A., Hall, M.A., Rehg, J.E., Yue, W., Yu, J., Zhang, L., Onciu, M.*, et al.* (2008). Selection against PUMA gene expression in Myc-driven B-cell lymphomagenesis. Mol Cell Biol *28*, 5391-5402.

Giuriato, S., Ryeom, S., Fan, A.C., Bachireddy, P., Lynch, R.C., Rioth, M.J., van Riggelen, J., Kopelman, A.M., Passegue, E., Tang, F.*, et al.* (2006). Sustained regression of tumors upon MYC inactivation requires p53 or thrombospondin-1 to reverse the angiogenic switch. Proc Natl Acad Sci U S A *103*, 16266-16271.

Guccione, E., Martinato, F., Finocchiaro, G., Luzi, L., Tizzoni, L., Dall' Olio, V., Zardo, G., Nervi, C., Bernard, L., and Amati, B. (2006). Myc-binding-site recognition in the human genome is determined by chromatin context. Nat Cell Biol *8*, 764-770.

Hanahan, D., and Weinberg, R.A. (2000). The hallmarks of cancer. Cell *100*, 57-70.

Hanna, J., Markoulaki, S., Schorderet, P., Carey, B.W., Beard, C., Wernig, M., Creyghton, M.P., Steine, E.J., Cassady, J.P., Foreman, R.*, et al.* (2008). Direct reprogramming of terminally differentiated mature B lymphocytes to pluripotency. Cell *133*, 250-264.

Hart, A.H., Hartley, L., Parker, K., Ibrahim, M., Looijenga, L.H., Pauchnik, M., Chow, C.W., and Robb, L. (2005). The pluripotency homeobox gene NANOG is expressed in human germ cell tumors. Cancer *104*, 2092-2098.

Hay, R.T. (2005). SUMO: a history of modification. Mol Cell *18*, 1-12.

Hermeking, H., Rago, C., Schuhmacher, M., Li, Q., Barrett, J.F., Obaya, A.J., O'Connell, B.C., Mateyak, M.K., Tam, W., Kohlhuber, F.*, et al.* (2000). Identification of CDK4 as a target of c-MYC. Proc Natl Acad Sci U S A *97*, 2229-2234.

Herold, S., Wanzel, M., Beuger, V., Frohme, C., Beul, D., Hillukkala, T., Syvaoja, J., Saluz, H.P., Haenel, F., and Eilers, M. (2002). Negative regulation of the mammalian UV response by Myc through association with Miz-1. Mol Cell *10*, 509-521.

Hong, H., Takahashi, K., Ichisaka, T., Aoi, T., Kanagawa, O., Nakagawa, M., Okita, K., and Yamanaka, S. (2009). Suppression of induced pluripotent stem cell generation by the p53-p21 pathway. Nature *460*, 1132-1135.

Jacobs, J.J., Scheijen, B., Voncken, J.W., Kieboom, K., Berns, A., and van Lohuizen, M. (1999). Bmi-1 collaborates with c-Myc in tumorigenesis by inhibiting c-Myc-induced apoptosis via INK4a/ARF. Genes Dev *13*, 2678-2690.

Jones, R.M., Branda, J., Johnston, K.A., Polymenis, M., Gadd, M., Rustgi, A., Callanan, L., and Schmidt, E.V. (1996). An essential E box in the promoter of the gene encoding the mRNA cap-binding protein (eukaryotic initiation factor 4E) is a target for activation by c-myc. Mol Cell Biol *16*, 4754-4764.

Juin, P., Hueber, A.O., Littlewood, T., and Evan, G. (1999). c-Myc-induced sensitization to apoptosis is mediated through cytochrome c release. Genes Dev *13*, 1367-1381.

Kaeser, M.D., and Iggo, R.D. (2002). Chromatin immunoprecipitation analysis fails to support the latency model for regulation of p53 DNA binding activity in vivo. Proc Natl Acad Sci U S A *99*, 95-100.

Kawamura, T., Suzuki, J., Wang, Y.V., Menendez, S., Morera, L.B., Raya, A., Wahl, G.M., and Izpisua Belmonte, J.C. (2009). Linking the p53 tumour suppressor pathway to somatic cell reprogramming. Nature *460*, 1140-1144.

Kessler, J.D., Kahle, K.T., Sun, T., Meerbrey, K.L., Schlabach, M.R., Schmitt, E.M., Skinner, S.O., Xu, Q., Li, M.Z., Hartman, Z.C.*, et al.* (2012). A SUMOylation-dependent transcriptional subprogram is required for Myc-driven tumorigenesis. Science *335*, 348-353.

Kim, J., Chu, J., Shen, X., Wang, J., and Orkin, S.H. (2008). An extended transcriptional network for pluripotency of embryonic stem cells. Cell *132*, 1049-1061.

Kouzarides, T. (2007). Chromatin modifications and their function. Cell *128*, 693-705.

Lawlor, E.R., Soucek, L., Brown-Swigart, L., Shchors, K., Bialucha, C.U., and Evan, G.I. (2006). Reversible kinetic analysis of Myc targets in vivo provides novel insights into Myc-mediated tumorigenesis. Cancer Res *66*, 4591-4601.

Li, H., Collado, M., Villasante, A., Strati, K., Ortega, S., Canamero, M., Blasco, M.A., and Serrano, M. (2009). The Ink4/Arf locus is a barrier for iPS cell reprogramming. Nature *460*, 1136-1139.

Luscher, B., and Vervoorts, J. (2012). Regulation of gene transcription by the oncoprotein MYC. Gene *494*, 145-160.

Marion, R.M., Strati, K., Li, H., Murga, M., Blanco, R., Ortega, S., Fernandez-Capetillo, O., Serrano, M., and Blasco, M.A. (2009). A p53-mediated DNA damage response limits reprogramming to ensure iPS cell genomic integrity. Nature *460*, 1149-1153.

Martinato, F., Cesaroni, M., Amati, B., and Guccione, E. (2008). Analysis of Myc-induced histone modifications on target chromatin. PLoS One *3*, e3650.

Matallanas, D., Romano, D., Yee, K., Meissl, K., Kucerova, L., Piazzolla, D., Baccarini, M., Vass, J.K., Kolch, W., and O'Neill, E. (2007). RASSF1A elicits apoptosis through an MST2 pathway directing proapoptotic transcription by the p73 tumor suppressor protein. Mol Cell *27*, 962-975.

Mateyak, M.K., Obaya, A.J., Adachi, S., and Sedivy, J.M. (1997). Phenotypes of c-Myc-deficient rat fibroblasts isolated by targeted homologous recombination. Cell Growth Differ *8*, 1039-1048.

Melino, G., Bernassola, F., Ranalli, M., Yee, K., Zong, W.X., Corazzari, M., Knight, R.A., Green, D.R., Thompson, C., and Vousden, K.H. (2004). p73 Induces apoptosis via PUMA transactivation and Bax mitochondrial translocation. J Biol Chem *279*, 8076-8083.

Ming, L., Sakaida, T., Yue, W., Jha, A., Zhang, L., and Yu, J. (2008). Sp1 and p73 activate PUMA following serum starvation. Carcinogenesis *29*, 1878-1884.

Okita, K., Ichisaka, T., and Yamanaka, S. (2007). Generation of germline-competent induced pluripotent stem cells. Nature *448*, 313-317.

Orkin SH, Hochedlinger K. Chromatin connections to pluripotency and cellular reprogramming. Cell. 2011 Jun 10;145(6):835-50.

Oskarsson, T., Essers, M.A., Dubois, N., Offner, S., Dubey, C., Roger, C., Metzger, D., Chambon, P., Hummler, E., Beard, P.*, et al.* (2006). Skin epidermis lacking the c-Myc gene is resistant to Ras-driven tumorigenesis but can reacquire sensitivity upon additional loss of the p21Cip1 gene. Genes Dev *20*, 2024-2029.

Pasi, C.E., Dereli-Oz, A., Negrini, S., Friedli, M., Fragola, G., Lombardo, A., Van Houwe, G., Naldini, L., Casola, S., Testa, G.*, et al.* (2011). Genomic instability in induced stem cells. Cell Death Differ *18*, 745-753.

Patel, J.H., Loboda, A.P., Showe, M.K., Showe, L.C., and McMahon, S.B. (2004). Analysis of genomic targets reveals complex functions of MYC. Nat Rev Cancer *4*, 562-568.

Pelengaris, S., Khan, M., and Evan, G. (2002). c-MYC: more than just a matter of life and death. Nat Rev Cancer *2*, 764-776.
Reavie L, Buckley SM, Loizou E, Takeishi S, Aranda-Orgilles B, Ndiaye-Lobry D, Abdel-Wahab O, Ibrahim S, Nakayama KI, Aifantis I. Regulation of c-Myc Ubiquitination Controls Chronic Myelogenous Leukemia Initiation and Progression. Cancer Cell. 2013 Mar 18;23(3):362-75.

Rosenwald, I.B., Rhoads, D.B., Callanan, L.D., Isselbacher, K.J., and Schmidt, E.V. (1993). Increased expression of eukaryotic translation initiation factors eIF-4E and eIF-2 alpha in response to growth induction by c-myc. Proc Natl Acad Sci U S A *90*, 6175-6178.

Seoane, J., Le, H.V., and Massague, J. (2002). Myc suppression of the p21(Cip1) Cdk inhibitor influences the outcome of the p53 response to DNA damage. Nature *419*, 729-734.

Shachaf, C.M., Kopelman, A.M., Arvanitis, C., Karlsson, A., Beer, S., Mandl, S., Bachmann, M.H., Borowsky, A.D., Ruebner, B., Cardiff, R.D*., et al.* (2004). MYC inactivation uncovers pluripotent differentiation and tumour dormancy in hepatocellular cancer. Nature *431*, 1112-1117.

Soucie, E.L., Annis, M.G., Sedivy, J., Filmus, J., Leber, B., Andrews, D.W., and Penn, L.Z. (2001). Myc potentiates apoptosis by stimulating Bax activity at the mitochondria. Mol Cell Biol *21*, 4725-4736.

Stahl, M., Dijkers, P.F., Kops, G.J., Lens, S.M., Coffer, P.J., Burgering, B.M., and Medema, R.H. (2002). The forkhead transcription factor FoxO regulates transcription of p27Kip1 and Bim in response to IL-2. J Immunol *168*, 5024-5031.

Staller, P., Peukert, K., Kiermaier, A., Seoane, J., Lukas, J., Karsunky, H., Moroy, T., Bartek, J., Massague, J., Hanel, F*., et al.* (2001). Repression of p15INK4b expression by Myc through association with Miz-1. Nat Cell Biol *3*, 392-399.

Steiner, P., Philipp, A., Lukas, J., Godden-Kent, D., Pagano, M., Mittnacht, S., Bartek, J., and Eilers, M. (1995). Identification of a Myc-dependent step during the formation of active G1 cyclin-cdk complexes. Embo J *14*, 4814-4826.

Strasser, A., Elefanty, A.G., Harris, A.W., and Cory, S. (1996). Progenitor tumours from Emu-bcl-2-myc transgenic mice have lymphomyeloid differentiation potential and reveal developmental differences in cell survival. Embo J *15*, 3823-3834.

Takahashi, K., Tanabe, K., Ohnuki, M., Narita, M., Ichisaka, T., Tomoda, K., and Yamanaka, S. (2007). Induction of pluripotent stem cells from adult human fibroblasts by defined factors. Cell *131*, 861-872.

Tanaka, H., Matsumura, I., Ezoe, S., Satoh, Y., Sakamaki, T., Albanese, C., Machii, T., Pestell, R.G., and Kanakura, Y. (2002). E2F1 and c-Myc potentiate apoptosis through inhibition of NF-kappaB activity that facilitates MnSOD-mediated ROS elimination. Mol Cell *9*, 1017-1029.

Tran, H., Brunet, A., Grenier, J.M., Datta, S.R., Fornace, A.J., Jr., DiStefano, P.S., Chiang, L.W., and Greenberg, M.E. (2002). DNA repair pathway stimulated by the forkhead transcription factor FOXO3a through the Gadd45 protein. Science *296*, 530-534.

Utikal, J., Polo, J.M., Stadtfeld, M., Maherali, N., Kulalert, W., Walsh, R.M., Khalil, A., Rheinwald, J.G., and Hochedlinger, K. (2009). Immortalization eliminates a roadblock during cellular reprogramming into iPS cells. Nature *460*, 1145-1148.

Vafa, O., Wade, M., Kern, S., Beeche, M., Pandita, T.K., Hampton, G.M., and Wahl, G.M. (2002). c-Myc can induce DNA damage, increase reactive oxygen species, and mitigate p53 function: a mechanism for oncogene-induced genetic instability. Mol Cell *9*, 1031-1044.

Vassilev, L.T., Vu, B.T., Graves, B., Carvajal, D., Podlaski, F., Filipovic, Z., Kong, N., Kammlott, U., Lukacs, C., Klein, C*., et al.* (2004). In vivo activation of the p53 pathway by small-molecule antagonists of MDM2. Science *303*, 844-848.

Verga Falzacappa, M.V., Ronchini, C., Reavie, L.B., and Pelicci, P.G. (2012). Regulation of self-renewal in normal and cancer stem cells. FEBS J *279*, 3559-3572.

Wang, P., Yu, J., and Zhang, L. (2007). The nuclear function of p53 is required for PUMA-mediated apoptosis induced by DNA damage. Proc Natl Acad Sci U S A *104*, 4054-4059.

Wernig, M., Meissner, A., Foreman, R., Brambrink, T., Ku, M., Hochedlinger, K., Bernstein, B.E., and Jaenisch, R. (2007). In vitro reprogramming of fibroblasts into a pluripotent ES-cell-like state. Nature *448*, 318-324.

Wong, D.J., Liu, H., Ridky, T.W., Cassarino, D., Segal, E., and Chang, H.Y. (2008). Module map of stem cell genes guides creation of epithelial cancer stem cells. Cell Stem Cell *2*, 333-344.

You, H., Pellegrini, M., Tsuchihara, K., Yamamoto, K., Hacker, G., Erlacher, M., Villunger, A., and Mak, T.W. (2006). FOXO3a-dependent regulation of Puma in response to cytokine/growth factor withdrawal. J Exp Med *203*, 1657-1663.

Yu, J., Vodyanik, M.A., Smuga-Otto, K., Antosiewicz-Bourget, J., Frane, J.L., Tian, S., Nie, J., Jonsdottir, G.A., Ruotti, V., Stewart, R.*, et al.* (2007). Induced pluripotent stem cell lines derived from human somatic cells. Science *318*, 1917-1920.

Yu, J., Yue, W., Wu, B., and Zhang, L. (2006). PUMA sensitizes lung cancer cells to chemotherapeutic agents and irradiation. Clin Cancer Res *12*, 2928-2936.

Yu, J., and Zhang, L. (2008). PUMA, a potent killer with or without p53. Oncogene *27 Suppl 1*, S71-83.

Yu, J., Zhang, L., Hwang, P.M., Kinzler, K.W., and Vogelstein, B. (2001). PUMA induces the rapid apoptosis of colorectal cancer cells. Mol Cell *7*, 673-682.

Zeller, K.I., Zhao, X., Lee, C.W., Chiu, K.P., Yao, F., Yustein, J.T., Ooi, H.S., Orlov, Y.L., Shahab, A., Yong, H.C.*, et al.* (2006). Global mapping of c-Myc binding sites and target gene networks in human B cells. Proc Natl Acad Sci U S A *103*, 17834-17839.

Zhao, Y., Yin, X., Qin, H., Zhu, F., Liu, H., Yang, W., Zhang, Q., Xiang, C., Hou, P., Song, Z.*, et al.* (2008). Two supporting factors greatly improve the efficiency of human iPSC generation. Cell Stem Cell *3*, 475-479.

Zindy, F., Eischen, C.M., Randle, D.H., Kamijo, T., Cleveland, J.L., Sherr, C.J., and Roussel, M.F. (1998). Myc signaling via the ARF tumor suppressor regulates p53-dependent apoptosis and immortalization. Genes Dev *12*, 2424-2433.

Zindy, F., Knoepfler, P.S., Xie, S., Sherr, C.J., Eisenman, R.N., and Roussel, M.F. (2006). N-Myc and the cyclin-dependent kinase inhibitors p18Ink4c and p27Kip1 coordinately regulate cerebellar development. Proc Natl Acad Sci U S A *103*, 11579-11583.

9498–9507 *Nucleic Acids Research, 2011, Vol. 39, No. 22* *Published online 10 August 2011*
doi:10.1093/nar/gkr638

Myc and PI3K/AKT signaling cooperatively repress FOXO3a-dependent PUMA and GADD45a gene expression

Stefano Amente[1], Jiyuan Zhang[1], Miriam Lubrano Lavadera[1], Luigi Lania[1], Enrico Vittorio Avvedimento[2] and Barbara Majello[1,*]

[1]Department of Structural and Functional Biology, University of Naples 'Federico II' 80126 Naples and [2]Department of Biology, Cellular and Molecular Pathology, 'L. Califano' University of Naples 'Federico II' 80131 Naples Italy

Received May 11, 2011; Accepted July 20, 2011

ABSTRACT

Growth factor withdrawal inhibits cell cycle progression by stimulating expression of growth-arresting genes through the activation of Forkhead box O transcription factors such as FOXO3a, which binds to the FHRE-responsive elements of a number of target genes such as PUMA and GADD45a. Following exposure of cells to growth factors FOXO3a-mediated transcription is rapidly repressed. We determined that repression correlates with activation of PI3K/AKT pathway leading to FOXO3a phosphorylation and release of FOXO3a protein from PUMA and GADD45a chromatin. We show here that Myc significantly and selectively contributes to repression of FOXO-mediated expression of PUMA and GADD45a. We found that in Myc deprived cells inhibition of PUMA and GADD45a following serum stimulation is impaired and that Myc does not interfere with p53 induction of PUMA transcription. We observed that following activation, Myc is rapidly recruited to PUMA and GADD45a chromatin, with a concomitant switch in promoter occupancy from FOXO3a to Myc. Myc recruitment stimulates deacetylation of Histone H3 and H4 and methylation of lysine 9 in H3 (H3K9me2) on both PUMA and GADD45 chromatin. These data highlight a Myc role on cell growth by selectively inhibiting FOXO3a induced transcription of PUMA and GADD45.

INTRODUCTION

FOXO transcription factors, through direct binding to the cognate FHRE sites, direct expression of gene targets governing cell cycle arrest, apoptosis, metabolism, differentiation and oxidative defense. FOXO factors are regulated through the phosphatidylinositol 3-kinase (PI3-K) pathway. In the absence of growth factors, FOXOs are localized to the nucleous and transcriptionally active (1–3). Activation of AKT in response to growth factor stimulation induces phosphorylation of FOXOs at three highly conserved serine and threonine residues (2). Because the PI3K-AKT axis is activated in virtually all human cancers, FOXO proteins result frequently inactivated in cancer cells (4) and murine genetic studies provided formal proof of the role of FOXOs in tumor suppression (5,6). Constitutive FOXO3a activation results in the repression of Myc target genes (6–8), suppression of Myc-driven lymphomagenesis and activation of cell cycle arrest and apopotsis in human renal cell carcinoma (6,9). FOXO-mediated inhibition of Myc-target genes appears to operate through induction of Mxi1-SRa and mir-145 (7,8). It has been suggested that FOXO3a and Myc might co-regulate a common set of targets through their recruitment to the respective cognate binding sites present on the same sequences. Accordingly, there is a significant overlap between FOXO3a and Myc targets including growth-promoting factors CyclinD2, CDK4, CyclinE2 (7) and growth-arrest factors such as PUMA (10), p27kip1 (11–14) and GADD45a (15,16) suggesting that FOXO3a and Myc might reciprocally regulate a common set of genes.

Here, we evaluate if Myc can interfere with FOXO3a-dependent transcription of two targets, the proapoptotic BBC3/PUMA (10) and the DNA damage-responsive GADD45a (15). Using a conditional Myc expression system, we determined that in response to serum withdrawal, PUMA and GADD45 expression is upregulated by FOXO3a-dependent activation. Following cell growth stimulation and Myc activation, we found that Myc is rapidly recruited to PUMA and GADD45a chromatin,

*To whom correspondence should be addressed. Tel: +39 081 679062; Fax: +39 081 679233; Email: majello@unina.it
Present address:
Zhang Jiyuan, Institute for Cancer Genetics, Herbert Irving Comprehensive Cancer Center, Columbia University, NY 10032, USA.

with a concomitant switch in promoter occupancy from FOXO3a to Myc. Myc recruitment significantly and selectively contributes to repression of FOXO-mediated expression of PUMA and GADD45a and its presence on both PUMA and GADD45 chromatin correlates with induction of histone repressive marks such as deacetylation of Histone H3 and H4 and methylation of lysine 9 in H3 (H3K9me2) at these targets.

MATERIALS AND METHODS

Cell culture and drugs

RAT1 cells expressing a 4-hydroxytamoxifen (OHT)-inducible MycER chimera (17), RAT1 and RAT-Myc$^{-/-}$ cells were cultured in DMEM medium supplemented with 10% fetal calf serum. Cells were made quiescent by contact inhibition followed by serum removal for 2 days. To induce entry into the cycle, synchronized growth-arrested cells were treated with OHT (1 μM) alone or OHT plus serum or serum alone as indicated in the text and harvested at the indicated times. The AKT-inhibitor LY294002 (10 mM) was added in the media where indicated. mRNA expression was quantified by qRT–PCR (see below) and compared to quiescent cells. mRNA levels were normalized to β-glucuronidase (GUS) mRNA levels (18,19). Growing RAT-MycER cells were treated with OHT for Myc induction (Myc) for 4 h. OHT-treated and control-untreated cells were incubated with CPT (12 mM for 4 h) or Nutlin-3 (10 mM for 4 h) and then PUMA and/or GADD45a mRNA levels were quantified by qPCR as described below.

Transfections and siRNA

To carry out transient transfection experiments in RAT1 and RAT-MycER cells (19), we used MicroPoRATor Digital Bio Technology, a pipette-type electroporation. Indicated plasmids, DNAs or siRNA were introduced into each 3×10^6 dissociated cells in 100 μl volume according to manufacturer's instructions. Pulse width was determined according to applied voltages: 1400 V, 30 ms, 1 pulse. Electroporated cells were then seeded into 100-mm culture dishes containing 5 ml of culture media. After 5 h of recovery, the cells were serum deprived for 48 h. For siRNA treatments, ON-TARGETplus SMARTpool (L-003282-00-0005) Myc; and ON-TARGETplus Non-targeting pool (D-001810-10-5) were obtained from Dharmacon. An amount of 100 nM, final concentration of the pools, was used for each transfection. Expression of proteins was determined by western blot. In transfection experiments, RAT-MycER cells were transfected with the 3 μg of FOXO3a-TM vector expressing a constitutively active FOXO3a by electroporation as described (19) after 5 h of recovery, the cells were serum deprived for 48 h and mRNA levels were evaluated 1 and 4 h after treatment with serum and OHT.

mRNA quantification by qPCR

cDNA was prepared from total RNA with the Quantitect Reverse Transcription Kit (Qiagen) according to manufactory instructions. Each sample was assayed in triplicate. Oligoprimers are described in Supplementary Data. The qPCR data were normalized to the expression of the housekeeping β-glucuronidase (GUS) gene and after normalization the data were presented as fold change relative to the 0 point.

Quantitative chromatin immunoprecipitation

Quantitative chromatin immunoprecipitation (qChIP) experiments were performed essentially as described (18,19). For qPCR, 3 μl out of 150 μl of immunoprecipitated DNA was used with primers described in Supplementary Data. ACHR promoter amplicon was used as negative control in all experiments. Normal serum and input DNA values were used to subtract/normalize the values from qChIP samples by using: % Input = $2^{DCt} \times 3$; DCt = Ct(input)-Ct(cIP) (18,19). qRT–PCR and qChIP data are presented

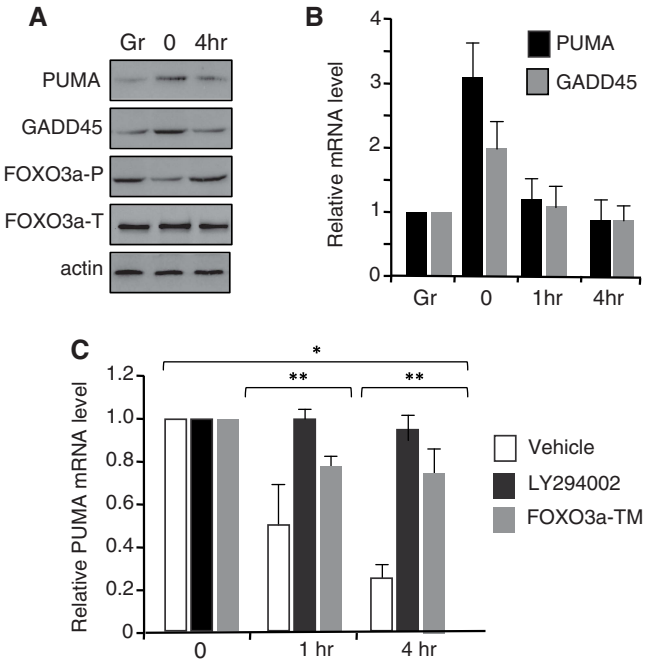

Figure 1. Myc inhibits FOXO3a-dependent transcription. Asynchronous RAT-MycER growing cells (Gr) were serum deprived for 2 days (0) and then treated with serum and OHT for 4 h. (**A**) Protein expression is shown in immunoblots of whole-cell extracts with anti-PUMA, anti-GADD45, anti-Phospho-FOXO3a, anti-FOXO3a and actin for loading control. (**B**) mRNA expression levels of PUMA and GADD45 were quantified by qRT–PCR in asynchronous RAT-MycER growing cells (Gr), quiescent (0) and after 1 and 4 h of treatment with serum and OHT. mRNA levels were normalized to β-glucuronidase (GUS) mRNA levels. All values represent the average of at least three independent experiments. Error bars indicate SD. (**C**) RAT-MycER cells were transfected with the FOXO3a-TM vector expressing a constitutively active FOXO3a by electroporation as described; after 5 h of recovery, the cells were serum deprived for 48 h and mRNA levels were evaluated 1 and 4 h after Myc induction in the presence of serum +OHT. The AKT-inhibitor LY294002 (10 mM) was added to the media where indicated. mRNA expression was quantified by qRT–PCR and compared to quiescent cells. mRNA levels were normalized to β-glucuronidase (GUS) mRNA levels. All values represent the average ± SD ($n = 3$). Error bars are standard error of the mean. $^*P < 0{\cdot}05$, $^{**}P < 0{\cdot}01$.

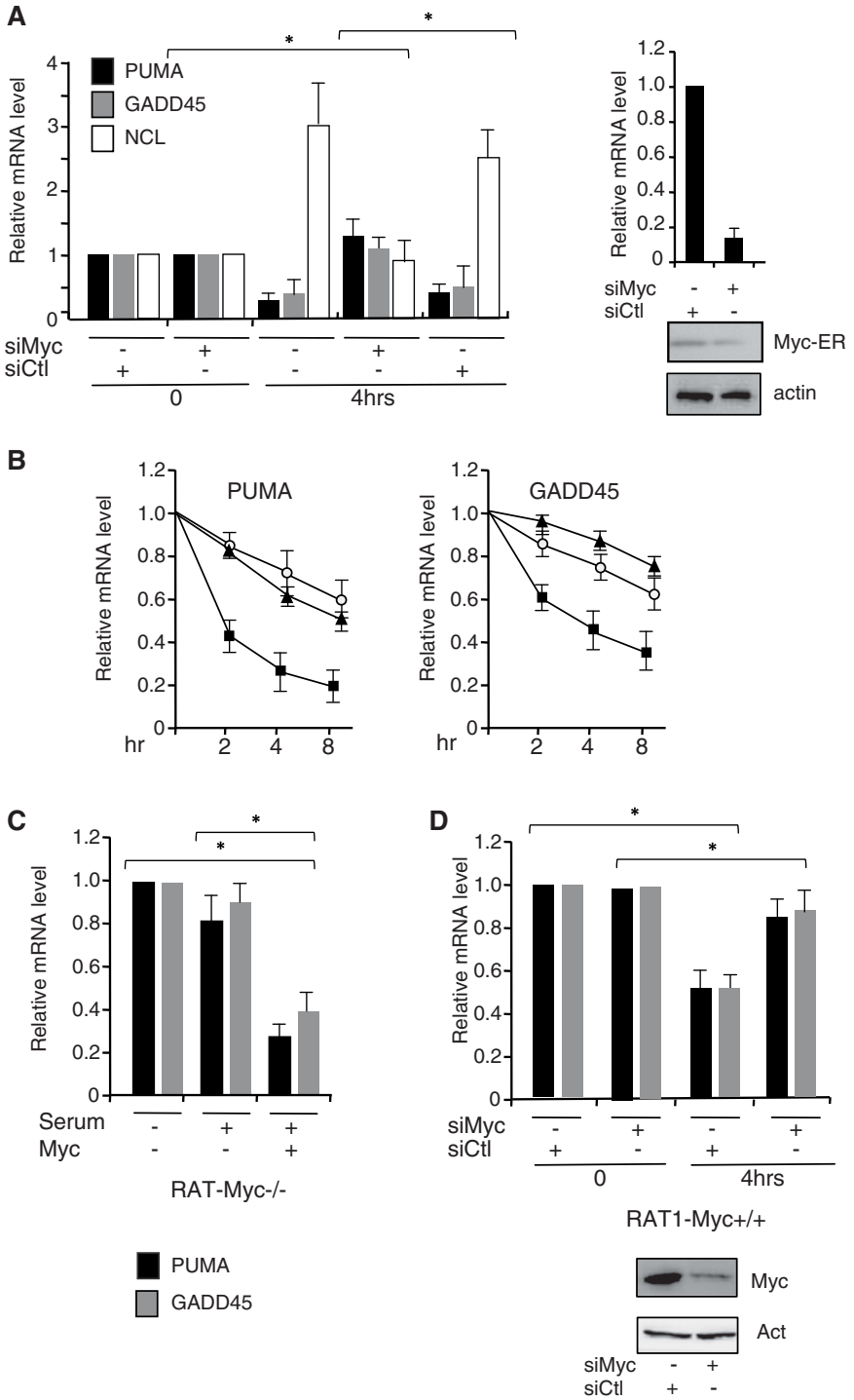

Figure 2. Myc knockdown prevents repression of FOXO3a targets. (**A**) Serum deprived RAT-MycER cells (0) were treated for 4 h with OHT^{+} serum. Myc expression was inhibited with specific siRNA (siMyc) and siRNA non-targeting (siCtl) was used as scrambled RNAs. PUMA, GADD45 and Ncl mRNAs expression levels were quantified by qRT–PCR. Error bars indicate SD ($n = 3$). Error bars are standard error of the mean. $^{*}P < 0{\cdot}05$. The efficiency of Myc silencing by siRNA treatments measured by qRT–PCR and by immunoblot is shown on the right. (**B**) Quiescent RAT-MycER cells were stimulated with OHT + serum (black square), with OHT alone (empty circle) or with serum alone (black triangles) and expression levels of PUMA and GADD45 were quantified by reverse transcription and real-time PCR at the indicated times after treatment; values were compared to quiescent cells and presented as means of two independent experiments each analyzed by triplicate qRT–PCR. (**C**) RAT-$Myc^{-/-}$ cells as well as cells transfected with a Myc expression vector were serum deprived for 48 h and PUMA and GADD45 mRNA levels were evaluated by qRT–PCR 4 h after serum induction. Values were compared to quiescent cells. (**D**) Serum deprived (2 days) RAT1 cells (O) were treated with serum (10%) for 4 h. Myc expression was inhibited with specific siRNA (siMyc) and siRNA non-targeting (siCtl) was used as scrambled RNAs. PUMA and GADD45 mRNAs expression levels were quantified by qRT–PCR. Error bars indicate SD ($n = 3$), $^{*}P < 0{\cdot}05$. The efficiency of Myc silencing by siRNA treatments measured by immunoblot is shown on the bottom.

as means of three at least independent biological experiments each analyzed by triplicate (±SD). Statistical significance was determined using the matched pairs test.

RESULTS

Myc contributes to repression of PUMA and GADD45 expression following growth stimulation

To investigate how Myc could influence FOXO3a-dependent transcription we used the RAT-MycER fibroblast cell line (18) in which the inducible MycER protein is activated upon treatment with tamoxifen (OHT). PUMA and GADD45a expression was monitored in asynchronous RAT-MycER cells, and in cells that were serum deprived for 2 days and then treated with OHT/serum for cell cycle reentry and Myc activation. As largely expected, PUMA and GADD45a expression is upregulated in response to growth factor deprivation, and addition of serum inhibits their expression (Figure 1A and B). In the absence of serum, the phosphoinositide 3-kinase PI3K/AKT pathway is inactive and FOXO3a remains unphosphorylated into the nucleus where it activates target genes (1,2). FOXO3a phosphorylation is inhibited by serum withdrawal and phosphorylation is restored 4 h after serum addition (Figure 1A). Moreover, the presence of the PI3-K inhibitor LY294002 or the overexpression of the constitutively active FOXO3a-TM, prevents PUMA and GADD45a repression by serum (Figure 1C). Collectively, these data indicate that activation of FOXO3a in serum-deprived RAT-MycER fibroblasts stimulates the expression of growth-arrested genes PUMA and GADD45a;

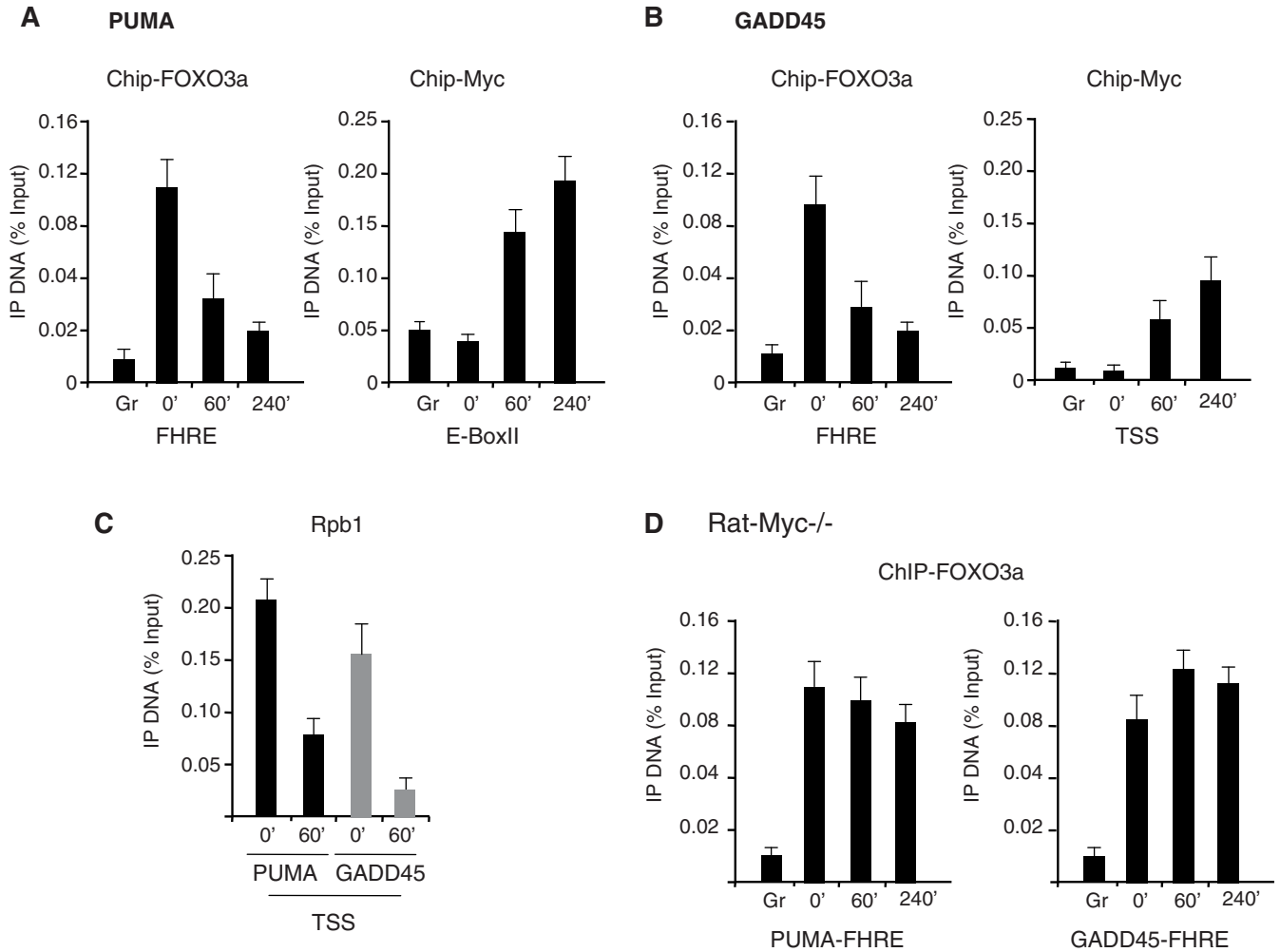

Figure 3. Myc, FOXO3a and Rpb1occupancy on PUMA and GADD45 chromatin. Asynchronous RAT-MycER growing cells (Gr) were serum deprived for 2 days (0′) and then treated with serum and OHT serum for Myc activation at the indicated times (30′, 60′ and 240′). qChIP was performed using antibodies recognizing FOXO3a (**A**), Myc (**B**) and Rpb1 (**C**). The amplicons used are reported in Supplementary Data. (**D**) FOXO3a occupancy on PUMA and GADD45 chromatin in growing (Gr) starved (0′) and serum treated (60′ and 240′) RAT Myc$^{-/-}$ cells. ChIP-enriched DNA was quantified by real-time PCR analysis using amplicons reported in Supplementary Data. The values reported were calculated as fold percentage of amount of immunoprecipitated DNA relative to that present in total input chromatin. All qChIP data are presented as mean of at least three independent biological experiments each analyzed by triplicate ± SDs. ACHR promoter amplicon was used as negative control in all experiments.

conversely, cell growth stimulation by serum is accompanied by repression of FOXO3a-dependent expression of these negative regulators of cell proliferation.

Because RAT-MycER cells express a conditional activated Myc protein, we sought to determine the relative contribution of Myc in the repression of FOXO3a target genes. We find that silencing of Myc with specific siRNA restores PUMA and GADD45a expression to levels comparable to that observed in serum-starved cells (Figure 2, panel A). As control, Myc silencing strongly reduces the expression of Nucleolin (NCL), a well-defined target for Myc activation (19). In serum-tarved cells, we did not detect significant differences on the relative levels of mRNA in samples treated with siCtl or siMyc, suggesting that in serum-starved cells, expression of both PUMA and GADD45 is largely independent from Myc. To determine the relative contribution of serum and Myc activation of the repression of PUMA and GADD5a, we compared the relative levels of expression in cells that were treated with serum alone, OHT and serum + OHT treatments. We found that Myc is able to repress FOXO3a-target genes even in the absence of serum, although under these conditions the kinetic of inhibition is slower (Figure 2B). On the other hand, serum does not fully substitute for Myc in the repression of PUMA and GADD45, because in RAT-Myc$^{-/-}$ cells serum addition does not fully repress FOXO3a-targets (Figure 2C); however, a robust repression of PUMA and GADD45a mRNA levels were restored in RAT-Myc$^{-/-}$ in which a Myc expression vector has been transfected (Figure 2C). To further investigate the endogenous Myc activity in response to serum addition, we monitored PUMA and GADD45a expression in RAT1 cells that were serum deprived for 2 days and then treated with serum for cell cycle re-entry. In response to serum addition expression of both PUMA and GADD45a was inhibited, and most importantly silencing of endogenous Myc with specific siRNA restores PUMA and GADD45a expression (Figure 2D). Collectively, these results highlight a crucial contributory role of Myc in the inhibition of FOXO3a-dependent gene expression in response to growth factor stimulation.

FOXO3a and Myc occupancy on PUMA and GADD45 chromatin is mutually exclusive

Previous works showed that Myc represses GADD45a through binding to the proximal promoter sequences (15,16), and several high affinity E-box sites for Myc binding have been mapped upstream the ATG site of PUMA (20–23), although a direct proof of Myc-binding to these putative E-boxes has not been documented.

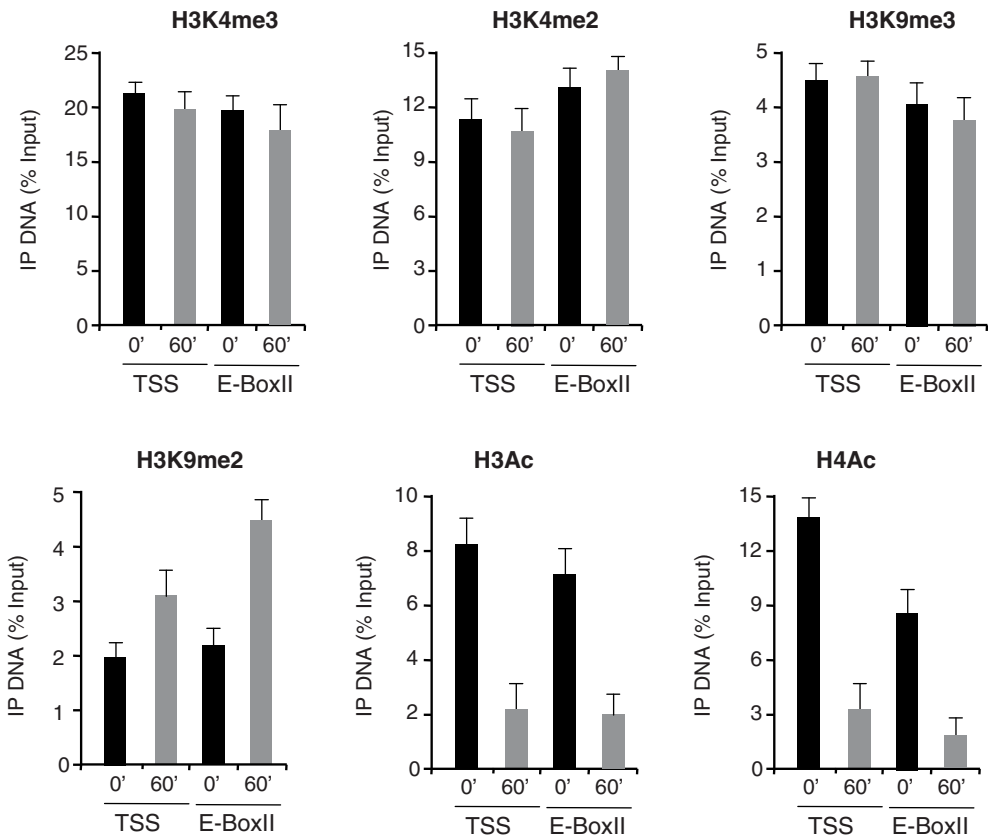

Figure 4. Histone modifications on PUMA chromatin following Myc activation. RAT-MycER serum starved cells (0′) are compared to cells induced with OHT and serum for Myc activation (60′). qChIP was performed using specific antibodies recognizing H3K4me3, H3K4me2, H3K9me3, H3K9me2, H3Ac and H4Ac as indicated. ChIP-enriched DNA was quantified by real-time PCR analysis using amplicons surrounding PUMA transcription start site (TSS) and E-BoxII (Supplementary Data). The qChIP data are presented as in Figure 3 and ChIP-enriched DNA was quantified as previously indicated.

Large-scale chromatin immunoprecipitation (ChIP) studies showed that PUMA contains high affinity E-box sites for Myc binding, suggesting that PUMA may represent a putative direct target of Myc. Moreover, clustering Myc target genes on the basis of histone modification marks, the PUMA E-boxes are characterized by high levels of histone methylation at H3K4me3, a pre-requisite for Myc binding and at H3K9me2, which is generally considered a repressive mark (24,25).

To assess Myc and FOXO3a occupancy on FOXO3a-targets (PUMA and GADD45) we carried out qChIP analysis in RAT-MycER growing cells (Gr), serum deprived for 2 days (0′) and treated for 60′ and 240′ with OHT/serum. First of all we determined that the PUMA E-boxII is the highest affinity Myc binding site and that Myc is recruited on this site rather early (60′) after induction (Supplementary Figure S1). Accordingly to the induction of expression of PUMA after serum withdrawal (Figure 1, panels A and B), recruitment of FOXO3a on the FHRE sequence is found in serum-starved cells (0′) (Figure 3A). As soon as Myc is recruited on E-BoxII chromatin, FOXO3a disappears on PUMA chromatin. Similar results are obtained by exploring GADD45 FHRE and TSS for Foxo3a and Myc occupancy (Figure 3B). These results indicate that upon cell cycle re-entry and Myc activation, there is a concomitant switch in promoter occupancy from FOXO3a to Myc resulting in transcriptional repression. Accordingly we also determined that the large subunit of RNAPII, Rpb1 occupancy at the transcription start sites of both PUMA and GADD45 is sharply reduced 60′ after Myc activation (Figure 3C). To address the relevance of serum on the reciprocal inhibition of binding to the chromatin of Myc and FOXO3a we performed a qChIP analysis in the RAT $Myc^{-/-}$ cells of FOXO3a occupancy in starved and serum-induced cells. As shown in Figure 3D, FOXO3a occupancy of the PUMA and GADD45a FHRE chromatin after 60′ and 240′ is slightly affected by serum addition compared to the strong reduction of FOXO3a observed in the presence of Myc, suggesting a causative role of Myc in the repression of FOXO3a-dependnet transcription.

Myc induces H3K9 methylation and H3–H4 de-acetylation on FOXO3a-targets chromatin

Myc responsive regions on the genome are characterized by specific histones marks (20–22). High affinity Myc binding sites are marked by tri-methylation of lysine 4 in the histone H3 tail. Upon Myc binding, changes in the methylation and acetylation levels of histones H3 and H4 have been correlated to the Myc positive or negative effects on transcription efficiency of its targets (26,27). We have performed qChIP assays to analyze histones

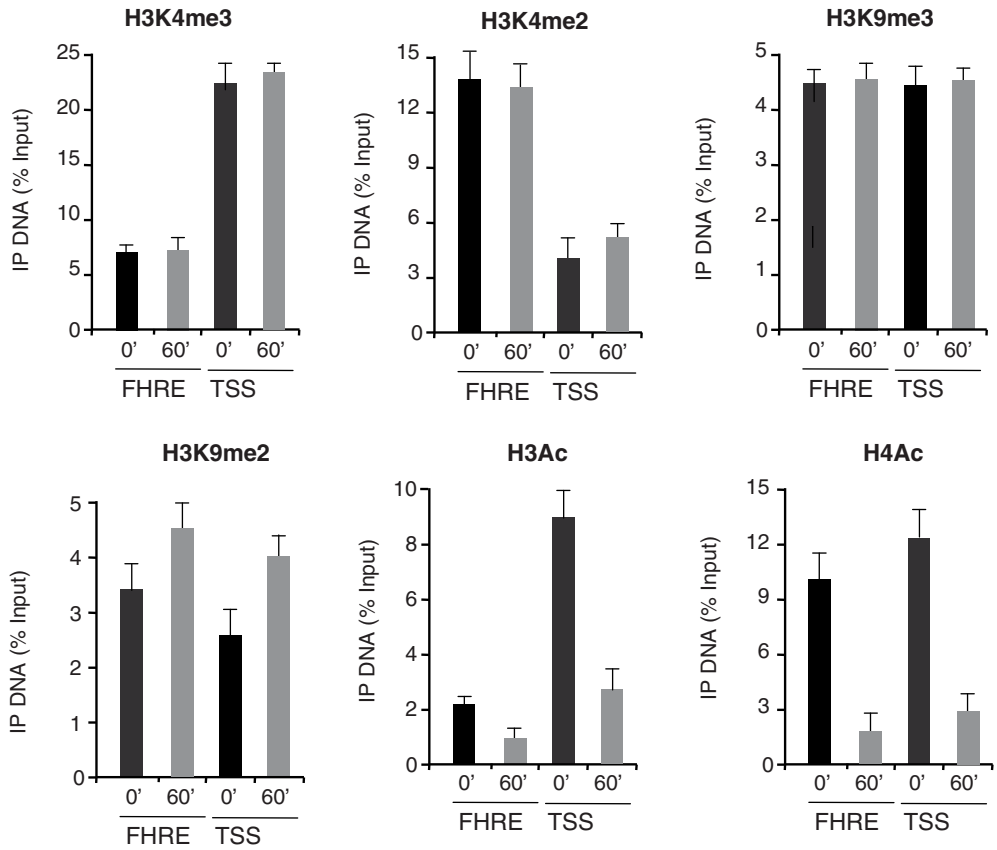

Figure 5. Histone modifications on GADD45 chromatin following Myc activation. RAT-MycER serum starved cells (0′) are compared to cells induced with OHT and serum for Myc activation (60′). qChIP was performed using specific antibodies recognizing H3K4me3, H3K4me2, H3K9me3, H3K9me2, H3Ac and H4Ac as indicated. ChIP-enriched DNA was quantified by real-time PCR analysis using amplicons (Supplementary Data) surrounding the TSS (−332) and FHRE (+23). The qChIP data are presented as described in Figure 3.

methylation and acetylation marks on PUMA TSS and E-boxII sequences (Figure 4) and on GADD45 FHRE and TSS sequences (Figure 5) following Myc binding. We have focused our attention on the methylation profile of lysine 4 and 9 of histone H3 and on pan-acetylation of histones H3 and H4. While H3K4me3, H3K4me2 and H3K9me3 levels remain largely unchanged, a robust increase of H3K9me2 is found on PUMA TSS and E-BoxII upon treatment with serum and MycER nuclear translocation by OHT treatment (Figure 4). Concurrent with Myc binding, we also detect a sharp reduction of H3- and H4-acetylated levels on PUMA TSS and E-BoxII sequences (Figure 4). Similar changes in chromatin modifications were found on the chromatin of GADD45 gene (Figure 5).

However, the combined treatment of RAT-MycER cells with OHT and serum does not allow to discriminate between the effects of Myc activation and serum-induced inactivation of FOXO3a. To define the relative contribution of Myc activation and serum, we carried out qChIP assays in RAT1 cells that only express the endogenous Myc analyzing histone modifications on GADD45 and PUMA chromatin in serum starved versus serum-treated cells. Comparing the ChIP data from RAT-MycER (Figures 4 and 5) with RAT1 cells (Figure 6 and Supplementary Figure S2) we find, as consequence of serum addiction to starved cells, a slower (4 h versus 1 h) reduction of acetylated H3/H4Ac (Figure 6A and B) on both PUMA and GADD45 chromatin (Supplementary Figure S2), and increased levels of methylation of H3K9 (Figure 6C) in the RAT1 cells. Furthermore, to support the relevant role of the endogenous Myc, we silenced Myc expression in RAT1 cells and, as shown in Figure 6, panel D, we find that the levels of H3 and H4 acetylation are largely unaffected in silenced cells, suggesting a causative role of Myc in the H3/H4 reduction following serum stimulation. To further support the role of Myc in the loss of H3 and H4 acetylation, we have used RAT $Myc^{-/-}$ cells to analyze H3/H4Ac occupancy on FOXO3a-targets. In this Myc null cell line, after 60′ and 240′ of serum starvation, H3/H4Ac occupancy of the both PUMA and GADD45 chromatin is largely unaffected, consistent with a relevant role of Myc in the reduction of H3- and H4-acetylated levels of both PUMA and GADD45 (Figure 7A). Finally, inhibition of histone deacetylases by TSA severely impairs Myc inhibitory effect on PUMA and GADD45 expression, following Myc induction (Figure 7B and C). These data indicate

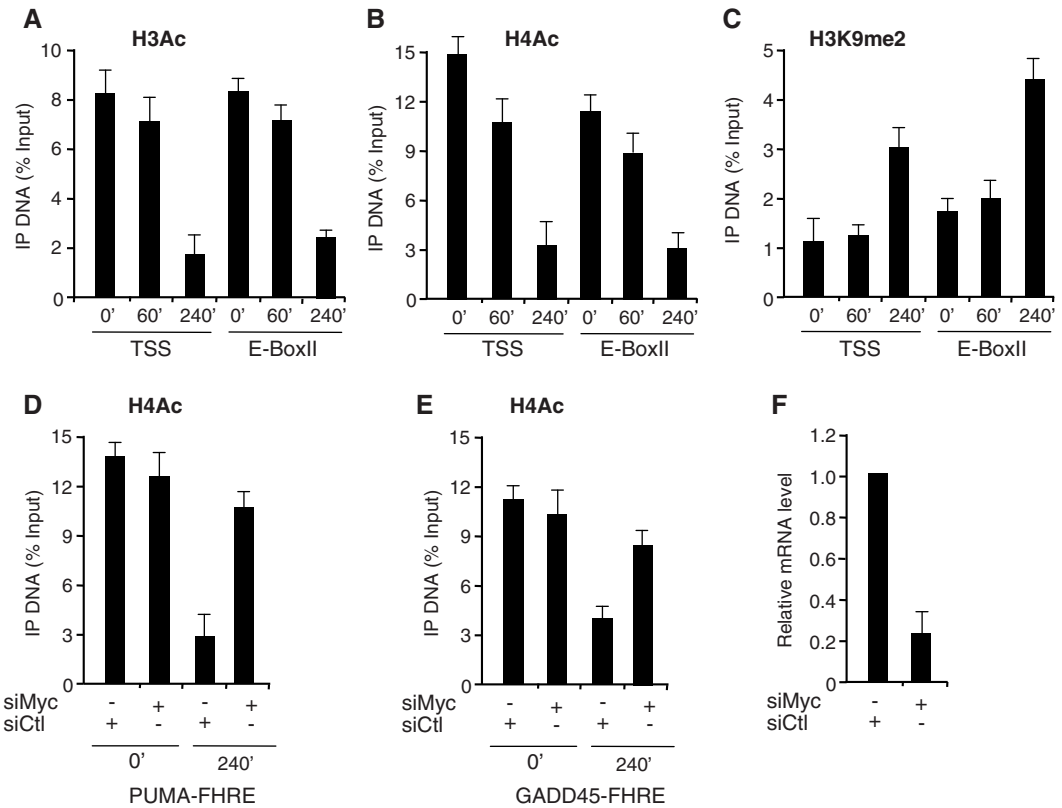

Figure 6. Myc is required for histone modification of PUMA chromatin. Asynchronous RAT1 growing cells were serum-deprived for 2 days (0′) and then treated with serum (10%) and samples collected at the indicated times (30′, 60′ and 240′) and qChIP was performed using specific antibodies recognizing H3Ac, H4Ac and H3K9me2, as indicated in panels **A**, **B** and **C**. ChIP-enriched DNA was quantified by real-time PCR analysis using amplicons surrounding PUMA, TSS and E-BoxII. The qChIP data are presented as in Figure 3. (**D** and **E**) Serum deprived (2 days) RAT1 cells (O) were treated with serum (10%) for 4 h. Myc expression was inhibited with specific siRNA (siMyc) and siRNA non-targeting (siCtl) was used as scrambled RNAs. qChIP was performed using antibody recognizing H4Ac, and ChIP-enriched DNA was quantified by real-time PCR analysis using amplicons surrounding PUMA and GADD45 TSS as indicated. Error bars indicate SD ($n = 3$). The efficiency of Myc silencing by siRNA treatments measured by qRT–PCR is shown in (**F**).

that Myc binding on PUMA and GADD45 regulatory regions correlates with increased methylation of H3K9 and with deacetylation of H3/H4.

Myc does not interfere with p53-mediated activation of PUMA

We sought to determine the specificity of Myc repressive effect on PUMA transcription independently from FOXO3a activation. PUMA expression following DNA damage is stimulated by p53 binding through consensus p53-responsive elements located within its promoter (23 and references therein). To determine whether Myc might suppress p53-mediated activation of PUMA, we analyzed the effect of Myc in the presence of active p53. p53 is activated by the DNA damaging compound Camptothecin (CPT) or by Nutlin-3, which disrupting p53-MDM2 interaction releases the active form of p53 (28). Asynchronous RAT-MycER growing cells were treated with CPT or Nutlin-3 for 4 h prior to Myc activation and PUMA mRNA levels were quantified by qRT–PCR (Figure 8A). Both CPT and Nutlin-3 treatments activate PUMA expression in the presence or absence of Myc. Next, we performed qChIP assays to analyze the occupancy of Myc and Rpb1 on PUMA regulatory regions following p53 activation by CPT and Nutlin-3. Figure 8B demonstrates that in condition in which CPT and Nutlin-3 activate PUMA, E-box occupancy by Myc is unaffected. Accordingly, TSS occupancy by Rpb1 in cells treated for p53 activation (CPT or Nutlin-3) remains unchanged after Myc activation (Figure 8C). These data demonstrate that Myc binding does not interfere with p53-mediated activation of PUMA and indicate that Myc is not a global repressor of PUMA expression.

DISCUSSION

In this report, we show that Myc and the PI3/AKT pathway cooperate in the repression of FOXO3a-dependent gene activation. Compelling evidences strongly suggest that Myc and PI3/AKT/FOXO3a pathways cooperate in the activation of Myc target genes, and abrogation of FOXO function promotes focus formation by Myc *in vitro*, and dramatically accelerates Myc-driven lymphomagenesis *in vivo* (7–9). Recent studies provided evidences that FOXO-mediated inhibition of Myc functions operates via suppression of Myc through upregulation of the Myc antagonists, Mxi1-SRa and mir-145 (6). The findings reported here suggest that the synergy between Myc and PI3/AKT/FOXO3a pathway has an

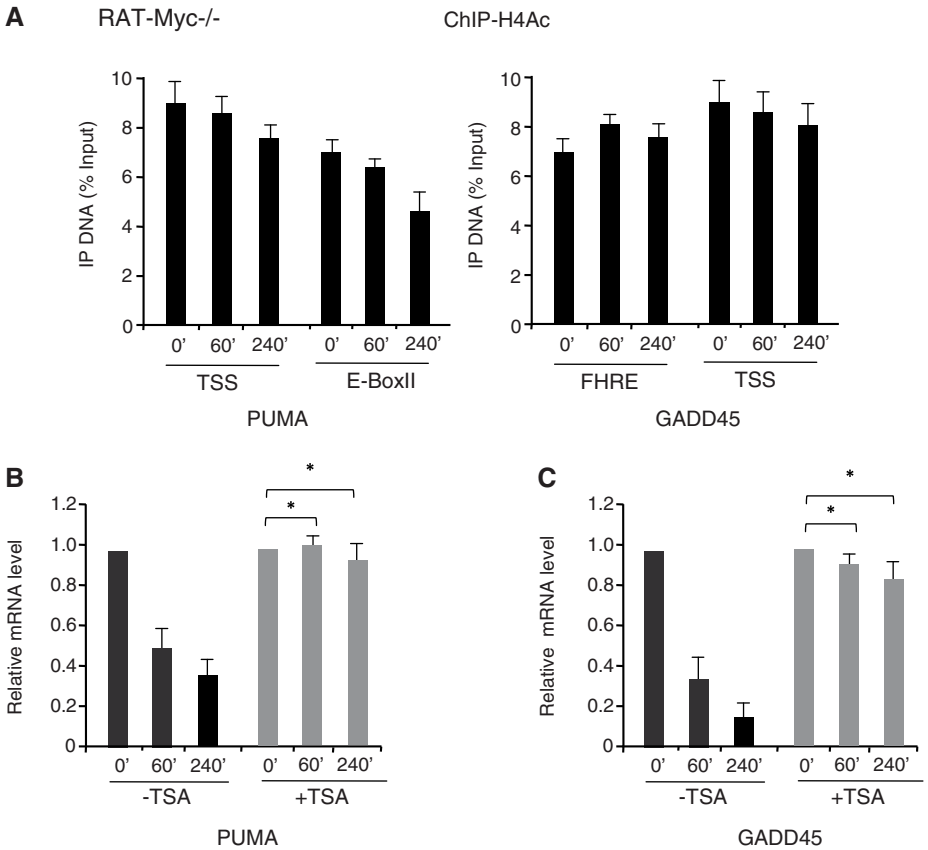

Figure 7. Histone H4 acetylation levels at Myc targets. (**A**) qChIP was performed using specific antibodies recognizing H4Ac in RAT-Myc$^{-/-}$-starved cells (0′) and treated with OHT and serum at the indicated times (60′, 240′). ChIP-enriched DNA was quantified as previously indicated. TSA impairs Myc inhibitory effect on PUMA (**B**) and GADD45 (**C**) activated transcription. Serum-deprived RAT-MycER cells (0) were treated for 60′ and 240′ with OHT^{+} serum in presence or absence of TSA (0.2 μg/ml) as indicated. PUMA and GADD45 expression levels were quantified by qRT–PCR. Error bars indicate SD ($n = 3$), $^{*}P < 0.01$.

important role not only in the activation of multiple Myc target genes involved in cell proliferation, but also in repression of FOXO3a targets involved in anti-proliferative function such as PUMA and GADD45a. Reciprocal control by Myc and FOXO3a has been also described in the regulation of p27Kip1transcription (11–13), and it has been suggested that Myc inhibits p27 transcription via physical association with FOXO3a (14). The presence of Myc on PUMA or GADD45a chromatin in the absence of FOXO3a, suggests that Myc recruitment does not rely on a physical FOXO3a/Myc interaction. Moreover, several attempts to detect interaction between Myc and FOXO3a using both endogenous and over-expressed proteins failed (data not shown), and we conclude that the divergent FOXO3a and Myc-mediated regulation of targets genes requires the recruitment of these factors in an independent and mutually exclusive manner. Indeed, there is a significant overlap between FOXO3a and Myc targets including growth-promoting factors CyclinD2, CDK4 CyclinE2 and growth-arrest factors such as PUMA, p27kip1 and GADD45a. It is highly suggestive that the opposite activity of FOXO3a and Myc proteins on common targets will profoundly affect the proliferation of normal and tumor cells (Figure 8D).

Our findings provide a mechanistic model for understanding the cooperation of Myc and PI3/AKT-signaling in repression of FOXO3a-dependent activation. First, in response to serum withdrawal PUMA and GADD45a are activated at transcriptional level and binding of active FOXO3a to the cognate FHRE sites is largely responsible for this effect. Serum external growth factors induce activation of the survival kinase AKT leading to phosphorylation of FOXO3a. However, AKT activation is not fully sufficient to repress FOXO-3a-dependent transcription. Myc binding to the FOXO3a targets further contributes to repression by establishing the repressive chromatin marks characterized by deacetylation of H3/H4 histones and increased levels of H4K9me2.

It has been recently reported that Myc-mediated repression of GADD153 and Id2 genes involves direct Myc binding to the E-box and a process that involves histone deacetylation (29). The findings reported here strongly

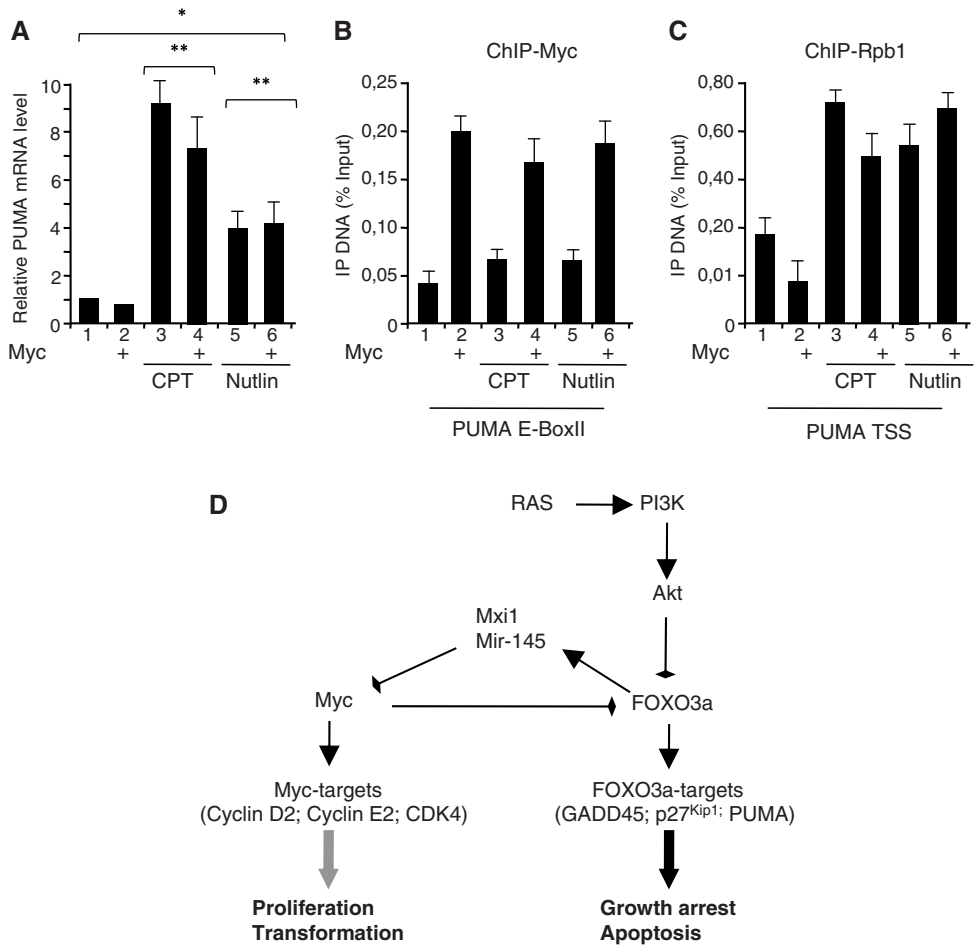

Figure 8. Myc does not repress p53-dependent PUMA activation. (**A**) Growing RAT-MycER cells were treated with OHT for Myc induction (Myc) for 4 h. OHT-treated and control-untreated cells were incubated with CPT (12 mM for 4 h) or Nutlin-3 (10 mM for 4 h) and then PUMA mRNA levels were quantified by qPCR as described in Figure 1. In parallel, recruitment of Myc (**B**) and Rpb1(**C**) on PUMA chromatin was determined by qChIP using the E-BoxII and TTS amplicons. All qChIP data are presented as mean of at least three independent biological experiments each analyzed by triplicate ± SDs, $*P < 0.05$, $**P < 0.01$. (**D**) Schematic model underlying the reciprocal role of Myc and FOXO3a in regulation of expression of growth promoting and growth arresting genes.

suggest that Myc-mediated repression of FOXO3a-dependent transcription correlates with induction of repressive epigenetic changes of target genes.

Following Myc activation, FOXO3a-mediated transcription is shut off and concurrently a robust increase of H3K9me2 (likely due to H3K9me1 methylation) and de-acetylation of H3 and H4 occurs on FOXO3a targets. Further investigations will be necessary to identify the H3/H4 de-acetylase and H3K9 methylase responsible of Myc mediated changes of FOXO3a target genes chromatin.

SUPPLEMENTARY DATA

Supplementary Data are available at NAR Online: Supplementary Figures S1–S2, Supplementary Methods.

ACKNOWLEDGEMENTS

The authors thank members of the laboratory for helpful discussion and suggestions.

FUNDING

Italian Association for Cancer Research (AIRC) (grant IG 5366); Italian Association for Cancer Research (to S.A.). Funding for open access charge: AIRC Grant.

Conflict of interest statement. None declared.

REFERENCES

1. Accili,D. and Arden,K.C. (2004) FoxOs at the crossroads of cellular metabolism, differentiation, and transformation. *Cell*, **117**, 421–426.
2. Brunet,A., Bonni,A., Zigmond,M.J., Lin,M.Z., Juo,P., Hu,L.S., Anderson,M.J., Arden,K.C., Blenis,J. and Greenberg,M.E. (1999) Akt promotes cell survival by phosphorylating and inhibiting a Forkhead transcription factor. *Cell*, **96**, 857–868.
3. Brunet,A., Sweeney,L.B., Sturgill,J.F., Chua,K.F., Greer,P.L., Lin,Y., Tran,H., Ross,S.E., Mostoslavsky,R., Cohen,H.Y. *et al.* (2004) Stress-dependent regulation of FOXO transcription factors by the SIRT1 deacetylase. *Science*, **303**, 2011–2015.
4. Fu,Z. and Tindall,D.J. (2008) FOXOs, cancer and regulation of apoptosis. *Oncogene*, **27**, 2312–2319.
5. Paik,J.H., Kollipara,R., Chu,G., Ji,H., Xiao,Y., Ding,Z., Miao,L., Tothova,Z., Horner,J.W., Carrasco,D.R. *et al.* (2007) FoxOs are lineage-restricted redundant tumor suppressors and regulate endothelial cell homeostasis. *Cell*, **128**, 309–323.
6. Gan,B., Lim,C., Chu,G., Hua,S., Ding,Z., Collins,M., Hu,J., Jiang,S., Fletcher-Sananikone,E., Zhuang,L. *et al.* FoxOs enforce a progression checkpoint to constrain mTORC1-activated renal tumorigenesis. *Cancer Cell*, **18**, 472–484.
7. Bouchard,C., Marquardt,J., Bras,A., Medema,R.H. and Eilers,M. (2004) Myc-induced proliferation and transformation require Akt-mediated phosphorylation of FoxO proteins. *EMBO J.*, **23**, 2830–2840.
8. Delpuech,O., Griffiths,B., East,P., Essafi,A., Lam,E.W., Burgering,B., Downward,J. and Schulze,A. (2007) Induction of Mxi1-SR alpha by FOXO3a contributes to repression of Myc-dependent gene expression. *Mol. Cell. Biol.*, **27**, 4917–4930.
9. Bouchard,C., Lee,S., Paulus-Hock,V., Loddenkemper,C., Eilers,M. and Schmitt,C.A. (2007) FoxO transcription factors suppress Myc-driven lymphomagenesis via direct activation of Arf. *Genes Dev.*, **21**, 2775–2787.
10. You,H., Pellegrini,M., Tsuchihara,K., Yamamoto,K., Hacker,G., Erlacher,M., Villunger,A. and Mak,T.W. (2006) FOXO3a-dependent regulation of Puma in response to cytokine/growth factor withdrawal. *J. Exp. Med.*, **203**, 1657–1663.
11. Dijkers,P.F., Medema,R.H., Lammers,J.W., Koenderman,L. and Coffer,P.J. (2000) Expression of the pro-apoptotic Bcl-2 family member Bim is regulated by the forkhead transcription factor FKHR-L1. *Curr. Biol.*, **10**, 1201–1204.
12. Stahl,M., Dijkers,P.F., Kops,G.J., Lens,S.M., Coffer,P.J., Burgering,B.M. and Medema,R.H. (2002) The forkhead transcription factor FoxO regulates transcription of p27Kip1 and Bim in response to IL-2. *J. Immunol.*, **168**, 5024–5031.
13. Chandramohan,V., Jeay,S., Pianetti,S. and Sonenshein,G.E. (2004) Reciprocal control of Forkhead box O 3a and c-Myc via the phosphatidylinositol 3-kinase pathway coordinately regulates p27Kip1 levels. *J. Immunol.*, **172**, 5522–5527.
14. Chandramohan,V., Mineva,N.D., Burke,B., Jeay,S., Wu,M., Shen,J., Yang,W., Hann,S.R. and Sonenshein,G.E. (2008) c-Myc represses FOXO3a-mediated transcription of the gene encoding the p27(Kip1) cyclin dependent kinase inhibitor. *J. Cell Biochem.*, **104**, 2091–2106.
15. Tran,H., Brunet,A., Grenier,J.M., Datta,S.R., Fornace,A.J. Jr, DiStefano,P.S., Chiang,L.W. and Greenberg,M.E. (2002) DNA repair pathway stimulated by the forkhead transcription factor FOXO3a through the Gadd45 protein. *Science*, **296**, 530–534.
16. Barsyte-Lovejoy,D., Mao,D.Y. and Penn,L.Z. (2004) c-Myc represses the proximal promoters of GADD45a and GADD153 by a post-RNA polymerase II recruitment mechanism. *Oncogene*, **23**, 3481–3486.
17. Littlewood,T.D., Hancock,D.C., Danielian,P.S., Parker,M.G. and Evan,G.I. (1995) A modified oestrogen receptor ligand-binding domain as an improved switch for the regulation of heterologous proteins. *Nucleic Acids Res.*, **23**, 1686–1690.
18. Gargano,B., Amente,S., Majello,B. and Lania,L. (2007) P-TEFb is a crucial co-factor for Myc transactivation. *Cell Cycle*, **6**, 2031–2037.
19. Amente,S., Bertoni,A., Morano,A., Lania,L., Avvedimento,E.V. and Majello,B. (2010) LSD1-mediated demethylation of histone H3 lysine 4 triggers Myc-induced transcription. *Oncogene*, **29**, 3691–3702.
20. Guccione,E., Martinato,F., Finocchiaro,G., Luzi,L., Tizzoni,L., Dall' Olio,V., Zardo,G., Nervi,C., Bernard,L. and Amati,B. (2006) Myc-binding-site recognition in the human genome is determined by chromatin context. *Nat. Cell Biol.*, **8**, 764–770.
21. Martinato,F., Cesaroni,M., Amati,B. and Guccione,E. (2008) Analysis of Myc-induced histone modifications on target chromatin. *PLoS ONE*, **3**, e3650.
22. Zeller,K.I., Zhao,X., Lee,C.W., Chiu,K.P., Yao,F., Yustein,J.T., Ooi,H.S., Orlov,Y.L., Shahab,A., Yong,H.C. *et al.* (2006) Global mapping of c-Myc binding sites and target gene networks in human B cells. *Proc. Natl Acad. Sci. USA*, **103**, 17834–17839.
23. Yu,J. and Zhang,L. (2008) PUMA, a potent killer with or without p53. *Oncogene*, **27(Suppl. 1)**, S71–S83.
24. Kouzarides,T. (2007) Chromatin modifications and their function. *Cell*, **128**, 693–705.
25. Cloos,P.A., Christensen,J., Agger,K. and Helin,K. (2008) Erasing the methyl mark: histone demethylases at the center of cellular differentiation and disease. *Genes Dev.*, **22**, 1115–1140.
26. Cowling,V.H. and Cole,M.D. (2006) Mechanism of transcriptional activation by the Myc oncoproteins. *Semin. Cancer Biol.*, **16**, 242–252.
27. Eilers,M. and Eisenman,R.N. (2008) Myc's broad reach. *Genes Dev.*, **22**, 2755–2766.
28. Vassilev,L.T., Vu,B.T., Graves,B., Carvajal,D., Podlaski,F., Filipovic,Z., Kong,N., Kammlott,U., Lukacs,C., Klein,C. *et al.* (2004) In vivo activation of the p53 pathway by small-molecule antagonists of MDM2. *Science*, **303**, 844–848.
29. Kurland,J.F. and Tansey,W.P. (2008) Myc-mediated transcriptional repression by recruitment of histone deacetylase. *Cancer Res.*, **68**, 3624–3629.

Am J Cancer Res 2012;2(3):330-334
www.ajcr.us /ISSN:2156-6976/ajcr0000109

Brief Communication

SUMO-activating SAE1 transcription is positively regulated by Myc

Stefano Amente, Miriam Lubrano Lavadera, Giacomo Di Palo, Barbara Majello

Department of Structural and Functional Biology, University of Naples 'Federico II', Naples, Italy.

Received February 7, 2012; accepted March 22, 2012; Epub April 21, 2012; Published May 15, 2012

Abstract: Myc protein plays a fundamental role in regulation of cell cycle, proliferation, differentiation and apoptosis by modulating the expression of a large number of targets. Here we report the transactivation ability of the human Myc protein to activate the SUMO-activating enzyme SAE1 transcription. We found that Myc activates SAE1 transcription via direct binding to canonical E-Boxes sequences located close to the SAE1 transcription start site. A recent report has highlighted the crucial role of the SAE gene expression in Myc mediated oncogenesis. Our study adds new insight in this context since we show here that Myc directly activates SAE1 transcription, suggesting that Myc oncogenic activity which depends on SAE1 is ensured by Myc itself through direct binding and transcriptional activation of SAE1 expression.

Keywords: Myc, SUMOylation, SAE1, transcription

Introduction

c-Myc is a regulatory gene that codes for a basic helix-loop-helix transcription factor (Myc) that can both activate and repress transcription. Myc activates transcription of dedicated target genes as component of the Myc/Max complex, which binds to specific DNA sequences, termed E-box [1, 2]. Oncogenic activation of Myc promotes regulation of a plethora of genes in the cell and the delicate balance of pro and anti tumorigenic properties of its targets defines the fate of the cells. Understanding the Myc-driven transcriptional program represent one of the most challenging aspect to decipher the molecular mechanisms underlying Myc-induced tumorigenesis [2, 3].

Here we report a novel and important target of Myc activity. We found that SAE1 transcription is activated by Myc through recruitment to E-box sequences located at SAE1 transcriptional start site. SAE1 in association with SAE2 form a critical component of the sole SUMO-activating enzyme necessary for SUMO conjugation to proteins [4]. SAE1 together with its partner SAE2/UBA2 has been recently shown to be necessary for the tumorigenicity of Myc-dependent cancer cells in vitro and in vivo [5], and most importantly gene expression analysis of Myc-high human breast cancer suggested that low SAE1/2 abundance in the tumors correlates with longer survival of the patients [5]. The findings reported here, showing that Myc directly activates SAE1 transcription, add new insight in this context, suggesting that Myc oncogenic activity which depends on SAE1 is ensured by Myc itself through direct binding and transcriptional activation of SAE1 expression.

Materials and methods

Cell culture and drugs

RAT1 cells expressing a 4-hydroxytamoxifen (OHT)-inducible MycER chimera and RAT-Myc-/- cells were cultured in DMEM medium supplemented with 10% fetal calf serum and MycER induction was carried out with OHT (1μM) as recently described [6, 7]. Cells were made quiescent by contact inhibition followed by serum removal for two days. To induce entry into the cycle, synchronized Go arrested cells were treated alone or OHT plus serum or serum alone as indicated in the text and harvested at the indicated times. Human retinal hT-RPE-MycER

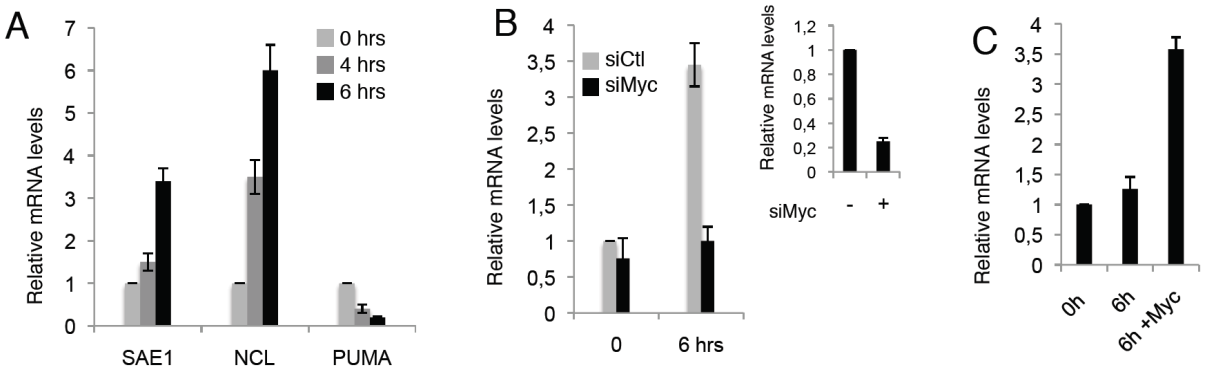

Figure 1. Myc activates SAE1 expression. (A) mRNA expression levels of SAE1, NCL and PUMA were quantified by qRT –PCR in quiescent cells (0) and after 4 and 6hrs of treatment with serum and OHT. (B) Myc expression was inhibited with specific siRNA (siMyc) and siRNA non-targeting (siCtl) was used as scrambled RNAs. SAE1 mRNAs expression levels were quantified by qRT–PCR in quiescent cells (0) and 6hrs of treatment with serum and OHT. The efficiency of Myc silencing by siRNA treatments measured by qRT–PCR is shown on the right. (C) RAT-Myc-/- cells as well as cells transfected with a Myc expression vector were serum deprived for 48 hrs. SAE1 mRNA levels were evaluated by qRT–PCR 6 hrs after serum induction. Values were compared to quiescent cells (0).

cell lines in which the inducible Myc-estrogen receptor fusion transgene (MycER protein) is activated upon treatment with tamoxifen (OHT) were grown and OHT-treated as recently described [8].

Transfections and siRNA

To carry out transient transfection experiments in RAT-Myc-/- and RAT-MycER cells, we used MicroPoRATor Digital Bio Technology, a pipette-type electroporation [6, 7]. Indicated plasmids, DNAs or siRNA were introduced into each $3X10^6$ -dissociated cells in 100-µl volume according to manufacturer's instructions. For siRNA treatments, ON-TARGETplus SMARTpool (L-003282-00-0005) Myc; and ON-TARGETplus Non-targeting pool (D-001810-10-5) were obtained from Dharmacon.

mRNA quantification by qPCR

cDNA was prepared from total RNA with the Quantitect Reverse Transcription Kit (Qiagen) according to manufactory instructions. Each sample was assayed in triplicate. The qPCR data were normalized to the expression of the housekeeping beta-glucuronidase (GUS) gene and after normalization the data were presented as fold change relative to the 0 point [6].

Quantitative chromatin immunoprecipitation (qChIP)

qChIP experiments were performed essentially as described [6, 7]. For qPCR 3µl out of 150µl of immunoprecipitated DNA was used with primers described in Supplementary Data. ACHR promoter amplicon was used as negative control in all experiments. Normal serum and input DNA values were used to subtract/normalize the values from qChIP samples by using: % Input = 2^{DCt}x3; DCt = Ct(input)-Ct(cIP). qRT-PCR and qChIP data are presented as means of three at least independent biological experiments each analyzed by triplicate (± SD).

Results and discussion

We have recently shown that the proapoptotic BBC3/PUMA (p53 up-regulated modulator of apoptosis) gene is a Myc target and through recruitment to an E-box binding site on its promoter, Myc cooperates with the PI3/AKT pathway to repress FOXO3a mediated activation of PUMA expression [7]. In the course of this study we were intrigued to observe a Myc responsive RNAPII peak in the second intron of PUMA locus in condition in which the PUMA expression was inhibited (data not shown). This finding prompted us to investigate the presence of actively expressed genes responsive to Myc activation in the region downstream of PUMA. Exploring the genomic region downstream of PUMA locus we found the presence of SUMO-activating enzyme SAE1 gene whose transcription proceeds in the opposite strand to PUMA.

To determine the expression of SAE1 in the presence of hyper-activated Myc protein, we

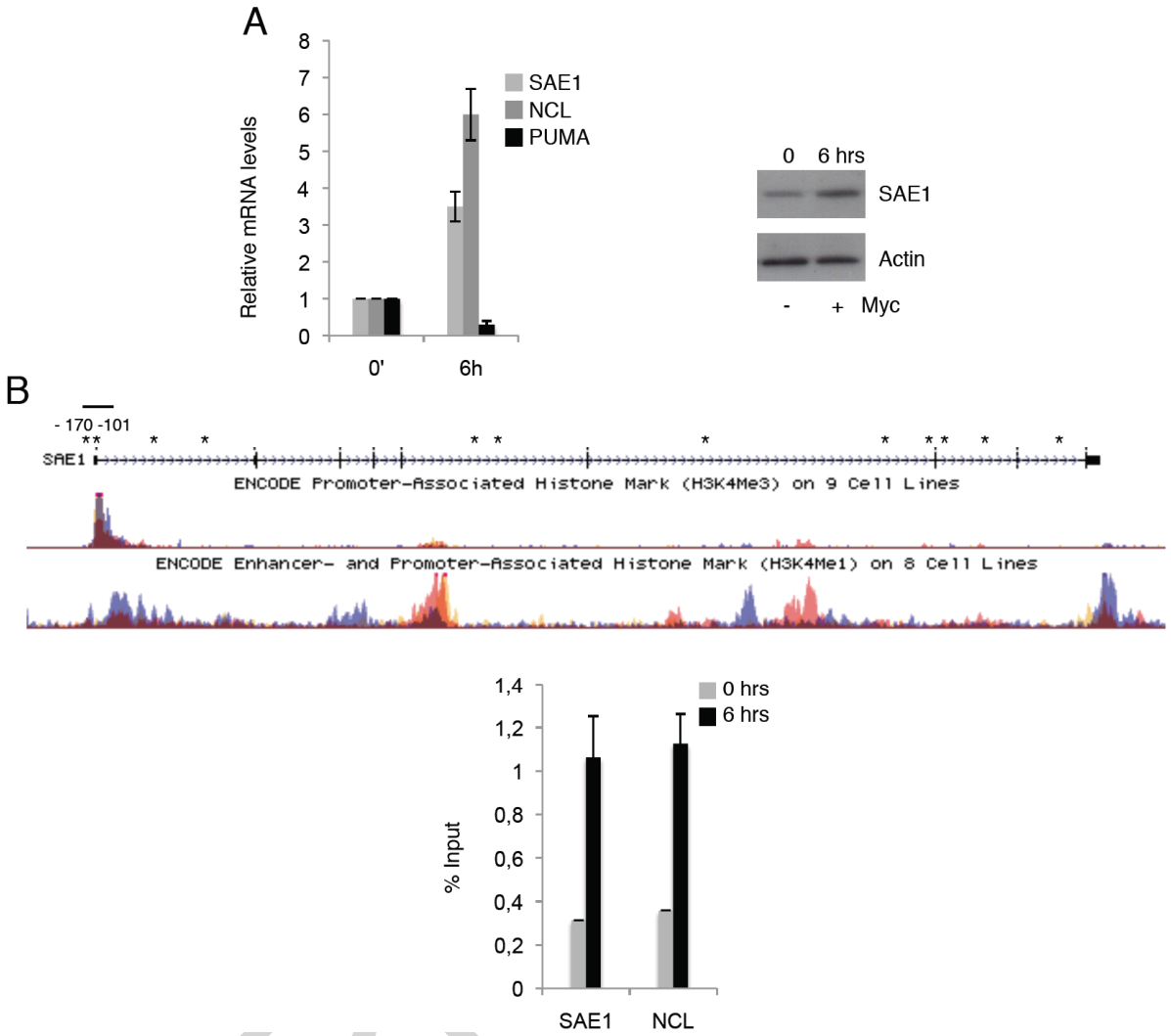

Figure 2. (A) hT-RPE-MycER cells were synchronized by 2 days of growth factors deprivation. SAE1, NCL and PUMA mRNAs expression levels were quantified by qRT–PCR in synchronized (0) and cells treated with growth factor + OHT (6hrs). All mRNA levels were normalized to β-glucuronidase (GUS) mRNA levels and all values represent the average of at least three independent experiments. Error bars indicate SD. Protein expression is shown in immunoblots of whole-cell extracts with anti-SAE1 and actin for loading control. (B) An adapted UCSC genome browser view of SAE1 genomic sequence displaying H3K4me3 and H3K4me1 levels and putative E-box (asterisks). Myc occupancy on SAE1 and NCL chromatin in synchronized (0) and Myc induced hT-RPE-MycER cells for 6hrs is shown. ChIP-enriched DNA was quantified by real-time PCR analysis using amplicon covering the region containing the Myc binding E-boxes as shown in Figure 2A.

used two Myc-inducible cell lines: the rat fibroblast RAT-MycER and the human retinal hT-RPE-MycER cell lines in which the inducible Myc-estrogen receptor fusion transgene (MycER protein) is activated upon treatment with tamoxifen (OHT) [6-8].

As shown in **Figure 1A**, in RAT-MycER, SAE1 expression as well as the known Nucleolin (NCL) Myc target, increase in response to Myc activation while the levels of expression of PUMA are inhibited as previously described [6]. To determine the contribution of Myc in the SAE1 activation we silenced Myc expression by transfection of specific siRNAs in the RAT-MycER cells and we found that Myc silencing inhibits activation of SAE1 transcription (**Figure 1B**). To further determine the contribution of Myc in SAE1 activation, we used the isogenic RAT-Myc$^{-/-}$ cells and measured SAE1 expression levels in

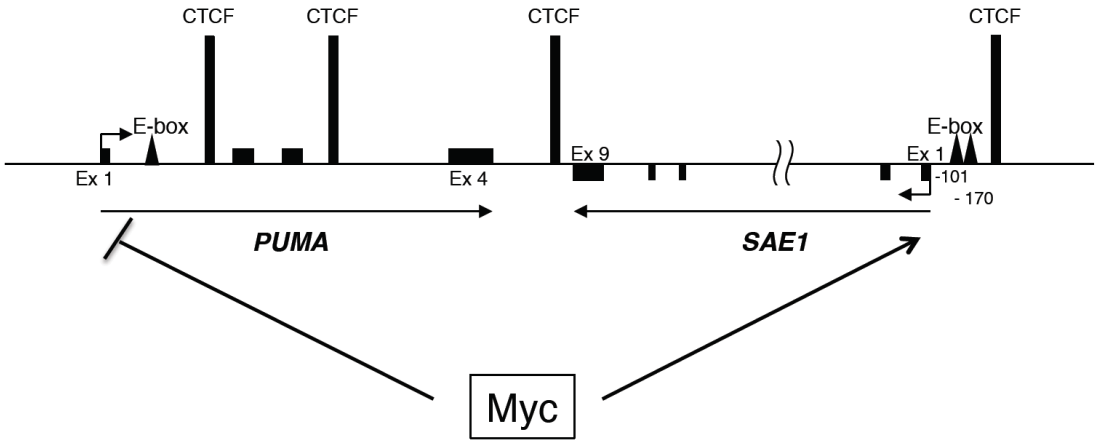

Figure 3. A general schematic of SAE1/*PUMA* locus showing CTCF binding sites and identified Myc binding sites (E-box).

starved versus serum-induced cells. As shown in **Figure 1C**, SAE1 expression slightly increases upon serum addiction while the expression was significantly higher when a Myc expression vector was introduced by transfection into RAT-Myc$^{-/-}$ cells. Collectively these results suggest that SAE1 expression is indeed regulated by Myc.

SAE1 sequence is extremely conserved between rat and human suggesting an evolutionary fundamental role in cell physiology. In this respect we analyzed SAE1 expression in the retinal human Myc inducible cell line hT-RPE-MycER [8] and, as shown in **Figure 2A**, Myc activation results in induction of SAE1 expression at levels comparable to the known Nucleolin (NCL), a well defined Myc target. To explore the role of Myc in SAE1 activation we scanned its genomic sequences for putative Myc binding sites. Several E-boxes were found, **Figure 2B**, and we focalized our attention on two closely associated E-boxes in position close to the TSS site (-170 and -101). Most importantly these E-boxes are located in a region with high level of H3K4Me3, a prerequisite for Myc binding (**Figure 2B**) [9, 10]. To assess Myc occupancy on SAE1 we carried out qChIP analysis in the RPE cells, which were growth factors-deprived for 2 days (0) and treated for 6hrs with OHT for Myc activation. Myc-immunoprecipitated chromatin was analyzed using amplicons spanning the SAE1 and NCL E-boxes and the qChIP data (**Figure 2B**) show that Myc is recruited on the E-box sites at the SAE1 promoter with efficiency comparable to recruitment on NCL. Although we cannot exclude the presence of additional E-box binding sites that might contribute to Myc activation, we can conclude that SAE1 is a bona-fide positively regulated Myc target through a direct binding to the E-boxes close to SAE1 TSS site.

While our studies on Myc role on SAE1 expression were in progress it has been reported the identification of genes vital to support Myc-addicted tumors through a genome wide genetic screen for Myc-synthetic lethal (MySL) shRNAs in human mammary epithelial cells [5]. The most significant candidates that have been isolated in this study are the SAE1 and SAE2 genes whose products associate to form the heterodimer that is a critical component of the SUMO activating enzyme needed for SUMO conjugation to proteins [4]. The authors found that SAE was required for growth of Myc dependent tumors and that the low expression of SAE1/2 in human breast cancers with high Myc expression levels correlates with longer survival of the patients. SAE depleted cells with high levels of Myc expression were found impaired in a correct mitotic spindle formation and consequently committed to apoptosis highlighting the crucial role of the SAE gene expression in Myc mediated oncogenesis.

Our study adds new insight in this context since we show here that Myc directly activates SAE1 transcription, suggesting that Myc oncogenic activity which depends on SAE1 is ensured by Myc itself through direct binding and transcriptional activation of SAE1 expression. Thus, recruitment of Myc on SAE1 modulates its expression supporting Myc oncogenic program by acti-

vation of Sumoylation dependent Myc-switchers (SMS genes).

Intriguing is the fact that the PUMA and SAE1 are adjacent on the human chromosome 19 and that their expression has been always found inversely correlated. While Myc cooperates with PI3/AKT pathway to repress PUMA transcription, hyper activation of Myc activates SAE1 transcription. An extensive analysis of chromatin domains at the PUMA locus and surrounding region including SAE1, has been recently provided by the Espinosa's laboratory [11, 12]. It has been identified a peculiar transcriptional organization of the locus with the presence of the insulator protein CTCF (CCCTC-binding factor) and the associated cohesin complex at intragenic PUMA as well as at intergenic regions between PUMA and SAE1 (**Figure 3**). Since CTCF functions involve the formation of 'chromatin loops' and these loops seems to be regulated in a signaling specific manner [13], it is possible that Myc binding might induce an intergenic gene looping between PUMA and SAE1 leading to the divergent Myc-mediated transcription control of SAE1 and PUMA loci. Further investigations will be necessary to validate these speculative hypotheses.

Acknowledgments

We thank L Lania for stimulating discussions and I Iaccarino for providing the hT-RPE-MycER cell line. This work was supported by a grant from MIUR (PRIN) to B.M.

Address correspondence to: Dr. Barbara Majello, Department of Structural and Functional Biology, University of Naples 'Federico II', Via Cinthia – 80126 Naples, ITALY Tel: (+) 39-081679062; Fax: (+) 39-081679233; E-mail: majello@unina.it

References

[1] Wasylishen AR, Penn LZ. Myc: The beauty and the beast. Genes and Cancer 2010; 1: 532-541.
[2] Meyer N, Penn LZ. Reflecting on 25 years with MYC. Nat Rev Cancer 2008; 8: 976-990.
[3] Eilers M, Eisenman RN. Myc's broad reach. Genes Dev 2008; 22: 2755-2766.
[4] Hay RT. SUMO. Mol Cell 2005; 18: 1-7.
[5] Kessler JD, Kahle KT, Sun T, Meerbrey KL, Schlabach MR, Schmitt EM, Skinner SO, Xu Q, Li MZ, Hartman ZC, Rao M, Yu P, Dominguez-Vidana R, Liang AC, Solimini NL, Bernardi RJ, Yu B, Hsu T, Golding I, Luo J, Osborne CK, Creighton CJ, Hilsenbeck SG, Schiff R, Shaw CA, Elledge SJ, Westbrook TF. A SUMOylation-dependent transcriptional subprogram is required for Myc-driven tumorigenesis. Science 2012; 335: 348-353.
[6] Amente S, Zhang J, Lubrano Lavadera M, Lania L, Avvedimento EV and Majello B. Myc and PI3K/AKT signaling cooperatively repress FOXO3a-dependent PUMA and GADD45a gene expression. Nucleic Acids Res 2011: 39: 9498-9507.
[7] Amente S, Bertoni A, Morano A, Lania L, Avvedimento EV and Majello B. LSD1-mediated demethylation of histone H3 lysine 4 triggers Myc-induced transcription. Oncogene 2010; 29: 3691-3702.
[8] Alfano D, Votta G, Schulze A, Downward J, Caputi M, Stoppelli MP and Iaccarinoi I. Modulation of cellular migration and survival by c-Myc through the downregulation of Urokinase (uPA) and uPA receptor. Mol Cell Biol 2010; 30: 1838-1851.
[9] Guccione E, Martinato F, Finocchiaro G, Luzi L, Tizzoni L, Dall' Olio V, Zardo G, Nervi C, Bernard L and Amati B. Myc-binding-site recognition in the human genome is determined by chromatin context. Nat Cell Biol 2006; 8: 764-770.
[10] Martinato F, Cesaroni M, Amati B and Guccione E. Analysis of Myc-induced histone modifications on target chromatin. PLoS One 2008; 3: e3650.
[11] Gomez NP, Espinosa JM. Disparate chromatin landscapes and kinetics of inactivation impact differential regulation of p53 target genes Cell Cycle 2010; 9: 3428-3437.
[12] Gomez NP, Espinosa JM. Gene-specific repression of the p53 target gene PUMA via intragenic CTCF-Cohesin binding. Genes Dev 2010; 24: 1022-1034.
[13] Hou C, Dale R and Dean A. Cell type specificity of chromatin organization mediated by CTCF and cohesion. Proc Natl Acad Sci USA 2010; 107: 3651-3756.